Summer 8-2014

Self-Assembled Gold Nanoplexes for Cancer-Targeted siRNA Delivery

Yongliang Shi
University of Southern Mississippi

The University of Southern Mississippi

SELF-ASSEMBLED GOLD NANOPLEXES FOR CANCER-TARGETED SIRNA DELIVERY

by

Yongliang Shi

A Thesis
Submitted to the Graduate School
of The University of Southern Mississippi
in Partial Fulfillment of the Requirements
for the Degree of Master of Science

Approved:

Dr. Faqing Huang
Committee Chair

Dr. Douglas Masterson

Dr. Yalin Guo

Dr. Maureen Ryan
Dean of the Graduate School

August 2014

ABSTRACT

SELF-ASSEMBLED GOLD NANOPLEXES FOR

CANCER-TARGETED SIRAN DELIVERY

by Yongliang Shi

August 2014

Through layer-by-layer method, the authors have constructed three Au nanoplexes: AuPEI/RNA/PEI, AuPEI/RNA/PEI-mPEG, and AuPEI/NA/PEI-PEG-FA. All the nanoplexes are characterized by UV-vis spectrometry, DLS, and zeta potential. The surface density of the first layer PEI and second layer RNA were also determined. Moreover, the Au nanoplexes can protect siRNA from RNase degradation and are stable in cell culture medium.

siGLuc-ppp, $ssRNA_{80}$, and siF17 were delivered by the assembled Au nanoplexes, and the results were analyzed by GLuc assay, TB assay, and Luciferase assay. In terms of RNA delivery, the Au nanoplexes AuPEI/RNA/PEI exhibited excellent gene silencing efficiency (or causing severe cell death) in the absence of the serum during the transfection. In terms of targeted delivery, PEGylation greatly reduces the nonspecific delivery of siRNA caused by AuPEI/siRNA/PEI. However, no apparent difference is found between AuPEI/RNA/PEI-mPEG and AuPEI/RNA/PEI-PEG-FA.

Fast fabrication, versatility, and ability for siRNA protection are the major characters of our new developed Au nanoplex system. The high gene silencing efficiency in the absence of serum makes it an excellent delivery agent for negative-charged macromolecules *in vitro*. However, the application of the system in targeted delivery needs more exploration.

ACKNOWLEDGMENTS

Foremost, I would like to express my sincere gratitude to my advisor, Dr. Faqing Huang, for offering me such a great opportunity to perform research, giving me valuable advice, and showing me what a real scientist is. Besides my advisors, I would like to thank my committee members, Dr. Masterson and Dr. Guo, for their guidance and insightful comments. Furthermore, I would like to thank Dr. Bai on the collaboration for the delivery of antivirus siRNA.

I also want to express my thanks to lab mate, Joseph Spangler, for his selfless helping.

Moreover, I want to acknowledge The University of Southern Mississippi, Department of Chemistry and Biochemistry, and National Institutes of Health for financial support.

Last but not least, I want to express great thanks to my parents and my wife for their unconditional love and support.

TABLE OF CONTENTS

LIST OF TABLES

Table

LIST OF ILLUSTRATIONS

Figure

LIST OF ABBREVIATIONS

ABC-transporter	ATP-binding cassette transporter
AuNP	gold nanoparticle
CBA-DAH-R	cystaminebisacrylamide-diaminohexane
CM	cysteamine capped
DMSO	dimethyl sulfoxide
DTT	dithiothreitol
EPR	enhanced permeability and retention
FA	folic acid
FCS	fetal calf serum
EGFP	enhanced green fluorescence protein
FITC	fluorescein isothiocyanate
FR	folate receptor
GFP	green fluorescent protein
GLuc	Gaussia luciferase
HA	hyaluronic acid
HD	hydrodynamic diameter
LbL	layer-by-layer
Luc	luciferase
MUA	11-mercaptoundecanoic acid
PAH-Cit	cis-aconitic anhydride-functionalized poly (allylamine)

PAMAM	polyamidoamine
PBLG	poly (γ-benzyl L-glutamate)
PEG	polyethylene glycol
PEI	polyethyleneimine
PLL	poly (L-lysine)
PSS	poly (styrene sulfonate)
PVP	poly (vinylpyrrolidone)
RES	reticuloendothelial system
RISC	RNA-induced silencing
ssRNA	single strand RNA
TB	toluidine blue
VEGF	vascular endothelial growth factor
WSLP	water soluble lipopolymer

CHAPTER I

INTRODUCTION

The Potential of siRNA for Cancer Therapeutics

Traditional Cancer Treatment and the Limitations

Cancer is the general name for a group of more than 100 diseases characterized by the uncontrolled growth and spread of abnormal cells. Although there are many kinds of cancer, they all start because abnormal cells grow out of control.[1] The American Cancer Society estimated that in 2013, about 1,660,290 new cancer cases are expected to be diagnosed, and about 580,350 Americans are expected to die of cancer. Cancer has already become the second most common cause of death, exceeded only by heart disease.[1]

Traditional treatment of cancer includes surgery, radiation, and chemotherapy. Unlike radiation and surgery that are considered as local treatments, chemotherapy, defined as the use of chemicals to treat disease cancer, is almost always used as a systemic treatment: the chemicals travel through the body to the cancer cells.[2] The benefits of systemic treatment are the rapid action and biodistribution as well as the wide application to the inaccessible tissues for local treatment. Therefore, more than 100 drugs are used today for chemotherapy, either alone or in combination with other drugs or treatment.[1]

Although widely used in cancer therapy, conventional chemotherapy, which utilizes small molecular drugs, is far from successful. This problem mainly derives from their lack of tumor selectivity or so-called selective toxicity of these agents.[3] When the drugs attack tumor cells, they cannot tell the difference between cells of normal tissues

and cancer cells. Therefore, they cause damage on both of them. The normal cells that are most likely to be damaged are those that divide rapidly: bone marrow/blood cells, cells of hair follicles, cells lining the digestive tract, and cells lining the reproductive tract.[1] As a result, patients getting chemotherapy suffer from various severe and painful side effects, such as nausea and vomiting, hair loss, fatigue, and damage to the heart, nervous system, and lungs.[1]

Resistance to traditional chemotherapy is another problem for the chemotherapy. When chemotherapy was first introduced into clinical practice by Gilman in the 1940s, resistance, as Paul Ehrlich said, had already followed as a faithful shadow.[4] They found the tumor did not respond to the chemotherapeutic agent any more when the third treatment was applied.[5] Since then, resistance to cancer chemotherapy becomes a common phenomenon, especially in progressive disease. The most major reason for the acquisition of multidrug resistance in cultured cancer cells was the expression of one or more energy-dependent drug efflux pumps, which can detect and eject anticancer drugs from cells.[6] For example, P-glycoprotein (permeability glycoprotein, abbreviated as P-gp), a well-characterized ATP-binding cassette transporter (ABC-transporter), is usually unregulated in many untreated, intrinsically drug-resistant tumors.[7] P-gp detects and binds hydrophobic natural-product drugs, such as doxorubicin, vinblastine, and antiarrhythmics[8], and then releases them into the extracellular space.[9] Other reasons for resistance include reduced uptake of the drugs, insensitivity to drug-induced apoptosis, and induction of drug-detoxifying.[6]

"Targeted cancer therapies" were then introduced to the cancer treatment. The concept involves the drugs or substances that can specifically target the tumor cells and

block the growth and spread of cancer. Two main strategies are utilized right now. One is called the "functionality-targeted" strategy, which target the key molecules in the specific novel pathway in the cancer cell. One famous example is the Gleevec that is used to treat certain types of leukemia. Another is called "ligand-targeted strategy," which take advantage of the overexpression of specific ligand in the cancer cell surface to deliver the drugs specifically to cancer cells. RNA interference (RNAi), the Nobel Prize-winning discovery in 2006, provides a brand new mechanism for the "functionality-targeted" strategy, and small interfering RNA (siRNA) is proposed as the next generation of anti-cancer drug. In the introduction, I will present the potential and limitations of siRNA and the current status of development of non-viral vectors for siRNA delivery. Finally, I will discuss a specific "ligand-targeted strategy," folate receptor mediated targeted delivery.

The Mechanism of RNAi

To this point, the picture about the RNAi mechanism becomes clear (shown in Figure 1). Combined with the later studies, the RNAi pathway was summed up as followed: the RNAi pathway located in the cytoplasm of the cell consists of two phases: the initiation phase (generation of effector molecules) and the subsequent effector phase (the actual RNAi mechanism). The effector molecules can be divided into two types: small interfering RNA (siRNA) and micro RNA (miRNA). In general, siRNA is a 21-23 nucleotides (nt) double-stranded RNA (dsRNA) with two nucleotide 3'- overhangs and micro RNA usually comprises 22 nt dsRNA segments. siRNA is produced from the cleavage of long dsRNA by Dicer (a multi-domain enzyme of the RNase III family) in the cytoplasm while microRNA is produced in the nucleus where endogenously encoded primary miRNA transcripts (pri-miRNA) are processed into precursor miRNA (pre-

miRNA) and then transported into the cytoplasm where it is cleaved by Dicer. In the effector phase/second stage, both of the siRNA and miRNA are unwound, and only single-stranded (antisense) siRNA or miRNA is assembled into RNA-induced silencing complexes (RISC). With its guidance, RISC targets its complementary mRNA. Another difference between siRNA and microRNA is whether they have perfect sequence complementarily with its target messenger RNA (mRNA). siRNA binds its target with a perfect match and induces site-specific cleavage of the mRNA while miRNA binds its targets with a typically imperfect match and induces translational repression rather than mRNA degradation. Both of the pathways result in the inhibition of protein synthesis.

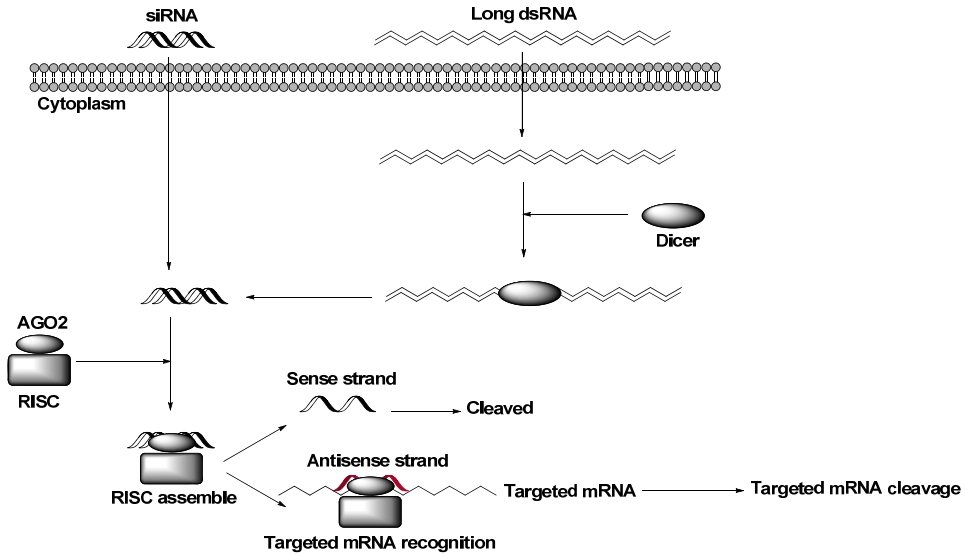

Figure 1. Mechanism of RNA interference.

Advantages and Challenges of RNAi-based Therapy

Shortly after the demonstration of sequence-specific knockdown in mammalian cell by synthetic siRNAs[10], McCaffey showed that they could also induce the suppression of the transgene expression in adult mice, and the specific and effective targeting of a sequence from hepatitis C virus by RNAi in vivo indicated the therapeutic potential of

this technique.[11] Since then, considerable efforts in the advancement of siRNA therapeutics were made for the treatment of various disease targets, including cancer.[12]

Firstly, siRNA has broader therapeutic potential than typical chemotherapy drugs. According to the RNAi mechanism, as long as the siRNA is designed appropriately, the RNAi machinery can be exploited to knock down any gene, expanding the universe of drugable targets to the entire genome.[13] For cancer, these genes include oncogenes/anti-apoptotic molecules or other survival factor, telomerase, growth factor receptor genes, key molecules in signaling pathways or genes essential for cell proliferation, and many of those are not considered viable conventional drug targets.[14] Moreover, these new types of drug targets could also, in principle, eliminate the cancer stem cells within a tumor or within other tumor cells that are relatively resistant to chemotherapy and radiation.[13]

The second reason is the high degree of specificity of siRNA targeting. Since many current drug targets are proteins with similar 3D structures, for example, the protein kinases, phosphatases and proteases, it is very difficult to develop small-molecular drugs that are specific for a single family member.

Despite the promise of RNAi for cancer therapy, some hurdles must be confronted to bring small RNAs into the clinic.

Systemic Elimination of siRNA

From the view of drug delivery, negative charges, large molecule weight and size, and instability of the naked siRNA molecules are unfavorable physicochemical properties which leads to short plasma half-life of <10 min.[15] Chemical modifications of the RNA backbone and the use of nano-sized carriers partially overcome these problems.[16]

Entrapment in reticuloendothelial system.[17] Since naked siRNA is seldom applied in systemic delivery, carrier systems are devised to protect siRNA from undesirable interaction with biological milieu components and from metabolism or degradation. However, after systemic administration, carriers are rapidly distributed to organs in the reticuloendothelial system (RES) and phagocytosed by the mononuclear phagocyte system, resulting in higher particle accumulations in RES organs, such as liver and spleen, relative to non-RES organs.

Vascular Endothelial Barrier.[18] Within an organ, siRNA or carriers undergo extravasation and enter the interstitium. Transport across vessel walls can occur via diffusion, convection through capillary pores, and transcytosis. In general, capillary pore size limits the upper size for the extravasated particulates. The pore size of tumor microvessels ranges from 100 to 780 nm in diameter. In comparison, microvessels in most normal tissues are less leaky. The tight junctions between endothelial cells are usually < 2 nm, and the pore size in post-capillary venules is < 6 nm, whereas fenestrated endothelium of the renal glomeruli and the sinusoidal endothelium of the liver and spleen show larger pore sizes of 40–60 and 150 nm, respectively. Due to vessel leakiness, the major pathway of drug transport across tumor microvascular wall is by extravasation via diffusion and/or convection through the discontinuous endothelial junctions, whereas transcytosis plays a relatively minor role.

Transport in Tissue Interstitium.[19] Transport of small molecules in the interstitial space is mainly by diffusion, whereas transport of large molecules is mainly by convection. Diffusion depends on the diffusivity and concentration gradient, and convection depends on the hydraulic conductivity and pressure difference. For tumors,

due to the higher interstitial fluid pressure compared to normal tissues, the pressure-driven convective flow in tumor interstitium is outward from the core of a tumor into the surrounding normal tissues. The lack of a lymphatic system in solid tumors increases interstitial fluid pressure, thereby inhibiting the convective transport in tumor interstitial space.

Internalization of siRNA in cells.[20] The major mode of internalization is endocytosis. The drug molecules are internalized together with a component of the cell membrane. Because of the high molecular weight, large size, and negative charges of the phosphate backbone, it is hard for naked siRNA to cross the anionic cell membrane by passive diffusion. The positively charged siRNA–carrier complex interacts with anionic proteoglycans on the cell surface, forms an endocytic vesicle, and enters the cells by endocytosis. Coating of carriers with ligands and antibodies can promote the carrier-specific binding to cell membrane.

Transport of siRNA within cells.[21] Following cellular internalization, the siRNA – carrier complex (in endocytic vesicles) is transported along microtubules to lysosomes. The fate of the internalized molecules inside the vesicle depends on the specific type of receptors and includes the following: recycled to the cell surface, degraded inside lysosomes, or released to other intracellular compartments including the cytosol. The endosomal entrapment and lysosomal degradation of siRNA-carrier contributes to the low transfection efficiency and is a major impediment for non-viral carriers.

Non-viral Vectors for siRNA Delivery

Viral vector based carriers and non-viral carriers are two main approaches to achieve cellular delivery of siRNA. The difference between the two is that viral vector-

based siRNA expressing cassettes provide a lasting RNAi effect, and non-viral systems only offer transient RNAi effects.[22] And the highly efficient delivery of the former make them the most powerful tools for transfection so far. However, their clinical application is limited by the invocation of immunogenic response, high cost of manufacturing, and the lack of cell specificity.[23] The following section mainly focuses on the non-viral carriers.

Polyethylenimine (PEI)

Polyethylenimine (shown in Figure 2), often considered the gold standard of gene transfection, is one of the most prominent examples of cationic polymers capable of gene transfection.[24]

In 1995, Behr first utilized branch PEI as the vector for gene and oligonucleotides transfer.[25] The motivation was that they were trying to look for a substitute that had similar DNA-condensing and pH-buffering properties to polyamidoamine (PAMAM) and lipopolyamines. PEI was selected due to its high cationic-charge-density and the buffering capacity at virtually any pH. Luciferase assay gave results comparable to or even better than lipopolyamines, and cytotoxicity was low and seen only at concentrations well above those required for optimal transfection. Combined with other results, the authors concluded that PEI was a promising vector for gene therapy and an outstanding core for the design of more sophisticated devices.[25]

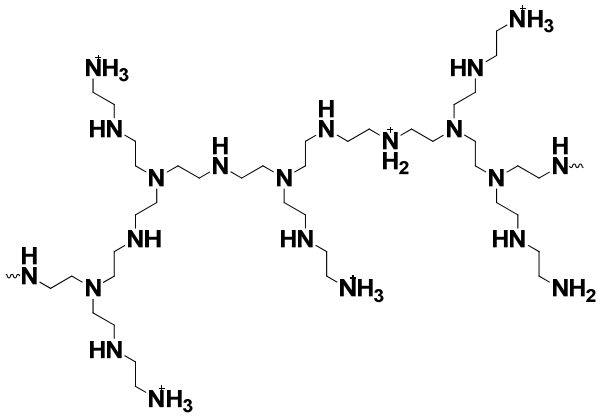

Figure 2. Chemical structure of PEI at neutral pH.

Two years later, Behr proposed "proton-sponge hypothesis" to explain the remarkable transfection properties of PEI.[26] The buffering capacity of PEI came from its unique structure: in every third position was an amino group so the overall protonation level increased from 20 to 45% between pH 7 and 5. Once the PEI/DNA complexes entered the cell by endocytosis, a high local concentration of PEI would be produced in the endosome. During the intracellular trafficking, the buffering capacity of PEI would inhibit the action of lysosomal nucleases that had an acid optimal pH and change the osmolarity of vesicle. The protons would also be accumulated. As a result, the ionic concentration within the endosome would increase considerably, which would result in the osmotic swelling of the endosome. Furthermore, the polymeric network would be expanded by the internal charge repulsion. Hence, the endosomal life would be greatly reduced, so the DNA would rapidly escape from the damaging endosomal environment.[26] By supported by further studies [27] [28], the theory has gained widespread acceptance despite challenges to the hypothesis.[24]

Effect of the Molecular Weight of PEI

The effect of the molecular weight and the size of PEI on the transfection efficiency were studied.[29] PEIs with nominal molecular weights of 600, 1200, 1800, 10,000, and 70,000 Da were examined at a pH of 5.0, 6.0, 7.0, and 8.0. They found the transfection efficiency was increased when the molecular weight of PEI increased. PEIs of lower molecular weights (< 1800 Da) produced no transfection at all. In contrast, the pH of the PEI solutions had no discernible effect on transfection.

The magnitude of the cytotoxic effect of PEI was found to be time and concentration dependent.[30] The molecular weight and the cationic charge density were the key parameters for interaction with cell membranes and consequently, the cell damage. High molecular weight polymers result in significantly higher cytotoxicity.[30] Hence, taking both efficiency and toxicity into consideration, the optimal molecular weight for PEI polyplex formation is typically between 5 and 25kDa.[31]

Effect of the Degree of Branching of PEI

In addition to molecular weight, the degree of branching of PEI could also influence the complex formation, transfection efficiency, and in vitro toxicity. Dunlap demonstrated that the branch form appeared to be a more effective condensing agent, compared with the linear PEI with similar molecular weight.[32] The binding ability and the complex stability could also be correlated with the number of primary amines, for they were highly protonated at a given pH.[33] [34] High branched PEIs achieve higher transfection efficiency due to the formation of smaller size of polyplexes but also possessed a higher toxicity.[35]

Functionalized PEIs

Various chemical modifications of PEI structure have been employed in an effort to reduce the cytotoxicity while maintaining or improving transfection efficiency (shown in Figure 3).

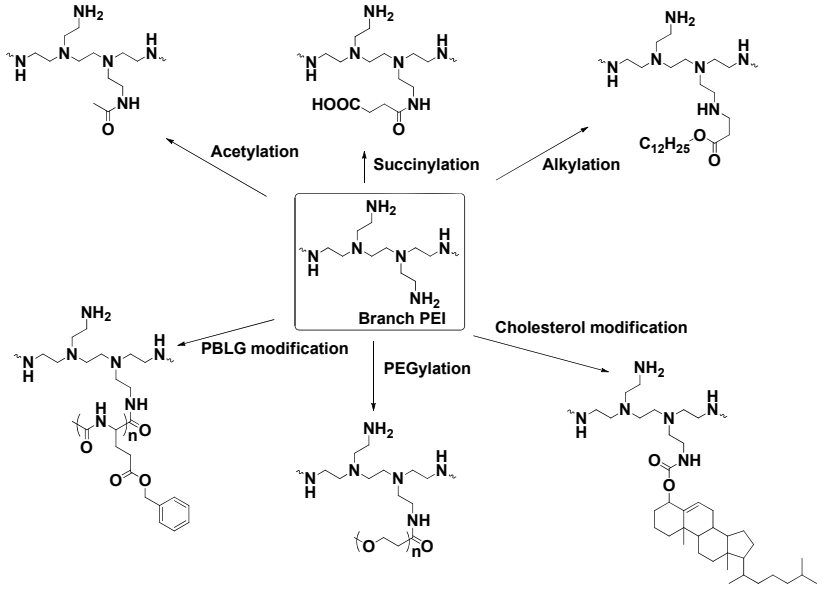

Figure 3. Various functionalized branched PEI.

With the initial purpose of investigating the effects of protonation properties of PEI, Forrest synthesized PEI derivatives by acetylating varying fractions of the primary and secondary amines to form secondary and tertiary amides.[36] Acetylation of PEI decreased the buffering capacity, zeta potential, and increased the diameter of the polyplex. Surprisingly, acetylation had a negligible effect on cytotoxicity of the polymers and increased gene delivery effectiveness by up to 21-fold compared to unmodified PEI, both in the presence and absence of serum.[36] Furthermore, Zintchenko introduced the negatively charged propionic acid or succinic acid group to the polymer structure.[37] Formulations of siRNA with succinylated PEI were able to induce remarkable knockdown of the target luciferase gene at the lowest tested siRNA concentration of 50

nM. In particular, succinylation of branched PEI resulted in up to 10-fold lower polymer toxicity in comparison to unmodified PEI.[37]

To combine the advantages of both liposomes and cationic PEI, Kim synthesized the water soluble lipopolymer (WSLP) which consisted of a positively charged head-group of low molecular PEI and hydrophobic lipid group of cholesterol.[38] The PEI component condenses DNA and enhances the transfection efficiency by escaping DNA complexes from degradative endosome or lysosome compartments, while the lipid coating on the complex increases its permeability through cell membranes. The WSLP showed low cytotoxicity and high transfection efficiency as compared with high-molecular-weight and non-modified PEI.[39] Borrowing the similar strategy, Philipp modified low molecular weight oligoethylenimine (OEI) with hydrophobic alkyl acrylates. The optimal structure was the conjugate containing ten hexyl acrylate residues per one OEI chain.[40] Chen designed and synthesized copolymer by grafting hydrophobic poly (γ-benzyl L-glutamate) segment (PBLG) to hyperbranched PEI, which exhibited lower cytotoxicity in comparison to unmodified PEI.[41]

It was well known that PEG (polyethylene glycol) could be used as a stabilized agent, which could shield the positive charge of the surface of the particles in order to avoid rapid systemic clearance. Hence, Mao synthesized PEI-graft-PEG block copolymer/siRNA polyplexes and investigated the effect of PEG chain length on their physicochemical and biological properties.[42] In agreement with their hypothesis, PEGylation could modify the stability of PEI/siRNA polyplexes. The release of siRNA in the cytosol depended on polyplex stability and protection against RNase digestion. A good correlation between RNase stability and knockdown efficiency in cell culture was

found for the polyplexes studied.[42] Further study showed that the optimal PEG-PEI-siRNA complex had a prolonged siRNA blood circulation time and reduced nonspecific uptake into the liver, spleen and lung as compared with those of non-PEGylated PEI-siRNA complex and naked siRNA.[39 43]

Bioresponsive Smart carrier system

As discussed above, both the efficacy and toxicity of PEI are strongly correlated with its molecular weight as well as the degree of branching. It seems that efficacy and side effects were strongly associated.[44] To close this gap, Berunig synthesized disulfide cross-linked low molecular-weight linear PEI/pDNA complexes (shown in Figure 4A) that were reductively degradable inside cells so that their charge density could be diminished to levels that minimized the risk of interactions with cellular components and therefore, exert significantly less toxicity.[44] Investigations with these materials revealed that the extracellular high MW provided outstandingly high transfection efficacies while the intracellular reductive degradation produced mainly nontoxic fragments. Compared with seven commercial transfection reagents in seven different cell lines, the degradable polymers showed highly superior transfection efficacies and substantially lower toxicities.[44]

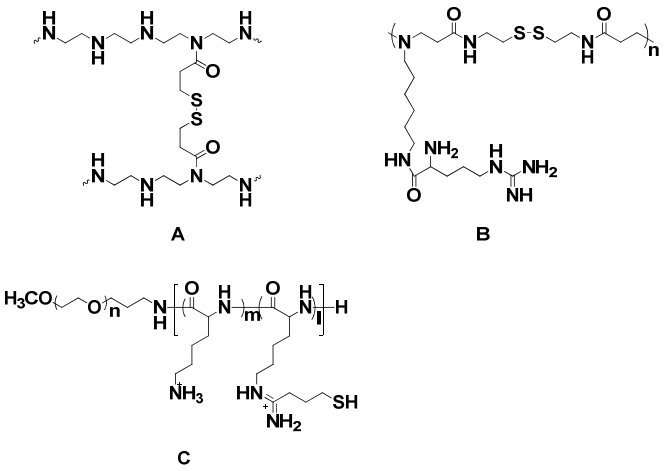

Figure 4. Structure of polycations bearing sensitive linkage for building smart carrier systems.

Borrowing the similar strategy, Kim synthesized a bio-reducible cationic polymer, arginine-conjugated poly (cystaminebisacrylamide-diaminohexane) (poly (CBA-DAH-R)) (shown in Figure 4B) as the siRNA carrier for therapeutic gene silencing for cancer.[45] After intracellular uptake of the siRNA/poly (CBA-DAH-R) polyplexes, the disulfide linkages in the polymeric backbone were cleaved in the reductive environment of the cytoplasm. As a result, the siRNA/poly (CBA-DAH-R) polyplexes were decomplexed, and siRNA molecules were released throughout the cytoplasm. With arginine modification, the siRNA/poly (CBA-DAH-R) polyplexes were demonstrated to possess increased membrane permeability and had a similar level of cellular uptake as siRNA/PEI polyplexes. However, the VEGF siRNA/poly (CBA-DAH-R) polyplexes, inhibited VEGF expression to a greater degree than VEGF siRNA/PEI in various human cancer cell lines due to the enhanced intracellular delivery and effective localization to the cytoplasm of the VEGF siRNAs.[45]

Another example that utilized the disulfide cross-linking was presented by Matsumoto.[46] They prepared a core-shell type polyion complex micelle with a disulfide

cross-linked core though the assembly of iminothiolane-modified poly (ethylene glycol)-block-poly (L-lysine) [PEG-b-(PLL-IM)] (shown in Figure 4C). The micelle was further mixed with siRNA at the optimum ratio. The resulting complexes showed a spherical shape of ~60 nm in diameter with a narrow distribution. The micellar structure was maintained at physiological ionic strength but was disrupted under reductive conditions due to the cleavage of disulfide cross-links, which is desirable for siRNA release in the intracellular reductive environment. And it was worth noting that environment-responsive micelles achieved 100-fold higher siRNA transfection efficacy compared with non-cross-linked PICs prepared from PEG-b-poly (L-lysine).[46]

Gold Nanoparticles

Gold nanoparticles (AuNPs) have a rich history in chemistry. As early as Roman times, people had used them to stain glasses for decoration. However, the modern era of AuNP synthesis actually started over 150 years ago.[47]

In 1857, Michael Faraday first synthesized colloidal gold by the reduction of gold chloride in the presence of sodium citrate, a stabilizing agent.[47] In the 1950s, these particles were found to bind protein biologics without altering their activity and were further used in handheld immunodiagnostics and in histopathology.[48] Later on, the radioactive colloidal AuNPs, made from Au^{198}, were used to treat liver cancer and sarcoma. Drug-associated toxicities were observed due to radiation exposure while no toxicities were noted form the particles themselves.[48] In the 1990s, AuNPs were assembled into macroscopic aggregates for DNA diagnostics and biosensor.[49]

In recent years, the unique chemical and physical properties of AuNPs are exploited for caner-selective photothermal therapeutics, non-invasive diagnostic imaging,

transporting, and unloading pharmaceuticals[50] [51]: 1) The strong resonant light-absorbing of AuNPs results in strong, highly localized photothermal heating upon laser illumination, an effect could be used to induce cancer cell death and tumor remission.[52] 2) The optical resonance of AuNPs could be tuned to any wavelength of interest by manipulating their shape and size.[52] 3) The spherical AuNPs were not inherently toxic to human cells, despite being taken up into cells.[53] 4) They are easily synthesized, and they are readily functionalized generally through thiol linkages.[51] 5) Their photophysical properties could trigger drug release at remote place.[54]

Layer-by-layer Approach for Assembly of AuNPs for siRNA Delivery

Lay-by-Layer (LbL) strategy was earlier utilized for fabrication of thin films on flat solid surfaces and microparticles. In 2009, Elbakry explored the feasibility of LbL to assemble AuNPs for siRNA delivery.[55] Shown in Figure 5, the AuNP/PEI/siRNA/PEI complex was prepared through deposition of oppositely charged polyelectrolytes layer by layer. The particles was characterized at each step, and the cellular uptake and gene silencing of the final particles were studied, providing valuable information to detect existing limitations and to design new materials for siRNA delivery.[55]

The author found that under appropriate polyelectrolyte concentration and ionic strength, the majority of AuNPs remained single particle. The hydrodynamic diameter of the intermediates and the final complex were smaller than 30 nm. After each coating, the AuNPs exhibited a charge reversal. The number of siRNA molecules was calculated to be around 780 siRNA molecules per particle. The further characterization of AuNPs in the serum-containing culture showed that the zeta potential of all particles types was

negative. The result of incubation of particles in the serum-free medium supported the hypothesis that serum proteins were necessary for stabilization of the nanoparticles.[55]

The study of cellular uptake of AuNPs showed that the number of siRNA/PEI-AuNPs per cell was 4 times more than that of PEI/siRNA/PEI, which suggested surface properties may strongly affect interactions with cells, for the AuNPs were of nearly similar size. However, in the gene silencing experiment, when siRNA was used as the top layer, no silencing efficacy was detected, while PEI/siRNA/PEI-AuNPs induced 72% knock-down efficacy of the cellular EGFP (enhanced green fluorescence protein) production. Finally, the cell viability assay showed PEI/siRNA/PEI-AuNPs had no serious toxicity in cell culture.[55]

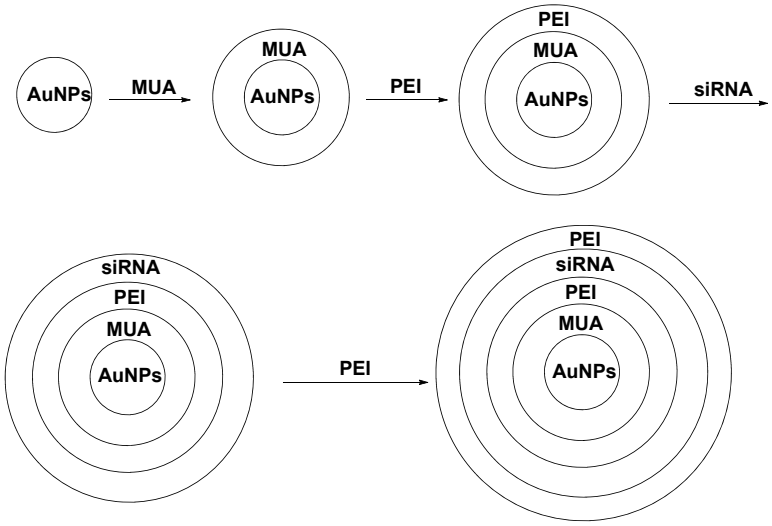

Figure 5. Flowchart illustrating the LbL deposition applied to AuNPs.

Later on, borrowing the LbL strategy, different forms of Au nanoparticles were synthesized: PEI capped AuNP/siRNA[56], cysteamine capped AuCM/siRNA/PEI/HA (HA = hyaluronic acid)[57], multilayered siRNA-coated AuNPs[58], and AuNP/PEI/PAH-Cit/PEI/siRNA (PAH-Cit = cis-aconitic anhydride-functinalized poly (allylamine)).[59] These systems can be divided into three groups by the surface properties: 1) the top layer

is positive charge polymer, for example, the multilayered siRNA-coated AuNPs, the top layer was PLL; 2) the top layer is siRNA, such as PEI capped AuNP/siRNA and AuNP/PEI/PAH-Cit/PEI/siRNA; 3) negative charged polymer: AuNP/siRNA/PEI/HA. Their physiochemical properties are summarized in Table 1.

Table 1

Characterization of Different AuNPs Complexes

Top layer	Positive charged polymer	siRNA		Negative charged polymer
	AuNP/PLL/siRNA/PLL/siRNA/PLL/siRNA/PLL	AuNP/PEI/siRNA	AuNP/PEI/PAH-Cit/PEI/siRNA	AuCM/siRNA/PEI/HA
H.D.	183 nm	51 nm/18 nm	Not available	166 nm
Zeta potential	40 mV	-16 mV/12 mV	Not available	-12 mV
siRNA per AuNP	Not available	Not available	Not available	44

H.D. = hydrodynamic diameter; AuCM = cysteamine capped AuNPs

Because of interparticle bridging and aggregation, the hydrodynamic diameter of the final AuNPs varied in a wide range. If we take a close look at the data they published (not shown in the table), we could find that when the AuNP was coated with siRNA layer, the size increased a lot: the diameter of AuNP/PLL/siRNA increased 60 nm, compared with AuNP; AuNP/PEI/siRNA with zeta potential of -16 mV increased 40 nm, in comparison with AuNP/PEI; AuCM/siRNA even increased 80 nm compared with AuCM alone. Although the above authors used the same strategy, the hydrodynamic

diameters were not consistent with each other. Besides, the siRNA per particles varied much too. It seemed that the positive charge surface could keep the AuNP remain single.

Biocompatibility and Biodistribution of AuNPs

When designing the anti-cancer AuNPs conjugates, stability is one significant aspect, for high ionic concentration are present in both physiologic fluids and cell growth media. The reason why the suspended AuNPs are relatively stable is that the working distance of their repulsive forces outweighs that of their attractive forces. Repulsive forces are generally determined by the surface charge of AuNPs (electrostatic repulsion) or related with physical separation, such as steric separation, while attractive forces are usually due to van der Waals interactions. In the physiological environment, electrostatic repulsion alone is often not enough to overcome Debye charge screening and subsequent nanoparticles aggregation. Therefore, to allow stable suspension of the particles in both high ionic strength and serum concentration environments, further surface modification of AuNPs is necessary.[50]

One strategy is to use the hydrophilic polymer to achieve physical separation. As mentioned above, PEG is the most common used surface ligand for stabilization and extended circulation time. Borrowing the same strategy, Maltzahn synthesized PEG-protected gold nanorods that exhibit superior circulation half-life in vivo as high as 17 h, compared with the prototypical particles.[60] Other common polymers used for physical isolation include poly (lysine) (PLL), poly-(styrene sulfonate) (PSS), and poly (vinylpyrrolidone) (PVP).[50]

When tumor cells grow to certain level, angiogenesis is induced for the tumor's requirements for a large amount of nutrition and oxygen. Compared with normal

vasculature, the blood vessels in the tumor are irregular in shape, dilated, leaky and defective, which further results in extensive leakage of blood plasma components, such as nanoparticles, into the tumor tissue. Because of the slow venous return in tumor tissue and the poor lymphatic clearance, the nanoparticles are retained in the tumor and then spread into tumor interstitium. This phenomenon is termed as the enhanced permeability and retention (EPR) effect.[57]

Of the tumor targeting, the EPR effect is a key mechanism for solid tumor targeting and considered a gold standard for novel drug design.[56] Based on this effect, anti-cancer gold nanoparticles conjugates could achieve size-selective accumulation at tumor sites. The optimal size depends on the stage, location, and type of cancer. Theoretically, the hydrodynamic diameter of a particle should be larger than 6 nm (renal clearance threshold) and smaller than 2 um.[50] Studies showed that gold nanoparticles exhibited 2-5% tumor accumulation by EPR effect.[50]

To maximally accumulate AuNPs in cells, Chithrani investigated the intracellular uptake of different sized and shaped colloidal AuNPs in cervical cancer cells.[61] They found the kinetics and saturation concentrations were highly dependent upon the physical dimensions of the nanoparticles (NPs), and 50 nm NPs had the shortest uptake half-life.[61]

In another study, Jiang studied how cells interacted with NP of a well-defined sized at the molecular level.[62] They showed that AuNPs coated with antibodies could regulate the process of membrane receptor internalization, and the binding and activation of membrane receptors strongly depended on their size. 40-and 50-nm NPs demonstrated the greatest effect.[62]

Moreover, NPs with positive surface charge could also promote the uptake because of the electrostatic attraction with anionic cell-surface proteolycans. However, similar to cationic lipoplexes and polyplexes, significant cytotoxicity was observed due to membrane disruption. Lipophilicity could also further promote the nanoparticles-cellular interaction and uptake but also resulted in poor aqueous stability and low circulatory half-life.[50]

Another key aspect in the design of anti-cancer gold nanoparticles conjugates is the pharmacokinetic clearance of circulating AuNP conjugates. Poly-anionic AuNPs up to 4-6 nm in hydrodynamic diameter typically exhibit efficient urinary excretion but often exhibit decreased cell penetration. Poly-cationic AuNPs with up to 6-8 nm in could be efficient cleared due to electrostatic attraction with the net negative charge of the capillaries. However, they have a poor circulatory half-life. When AuNPs were neutral in zeta potential and contained hydrophilic polymers such as PEG, they exhibited the lowest opsonizaiton and phagocytic uptake.[50]

Application of AuNPs in Cancer Therapeutics

Giljohann et al. attached siRNA directly to the surface of AuNPs via an PEG-thiol, and the conjugate had an inhibitory effect on luciferase expression in a luciferase-expressing cell line.[63] Lee et al. also directly attached siRNA to AuNPs and further modified the conjugate with poly (b-amino ester) to convey positive charge and enhance cellular uptake.[64] Recently, Braun et al. developed a near-infrared laser-controlled siRNA-release AuNP, which involved three layers: AuNP was firstly coated with thiol-PEG conjugated to siRNA, secondly covered with lipid, and thirdly decorated with TAT-

lipid. Laser irradiation cleaved the attachment of the thiol on the AuNP surface, so siRNA was released from AuNP depending on the intensity of the laser irradiation.

Folate-mediated Delivery

Two strategies for tumor-targeted therapies: the first one is to selectively block novel pathways or proteins that emerge or become over-expressed in malignant cells; the second one involves the use of a homing ligand that binds specifically to a receptor that is expressed primarily on malignant cells.[65]

Ligand-targeted therapies offer several advantages over the aforementioned functionality-targeted therapies, the most notable being the remarkable flexibility and adaptability. Almost any potent drug can be targeted to a tumor tissue if it can be linked reversibly to a targeting ligand with specificity for a pathologic cell type.[65]

Folic acid (FA) is a vitamin that is essential for the proliferation and maintenance of all cells. There are two mechanisms for the cells to internalize the folic acid[66 67]: direct transport[68] and endocytosis.[68 69] The expression of folate receptor (FR) isoforms (FR-α and FR-β) depends on tissues and differentiation states.[70 71]

Normal tissues usually do not express detectable FR[72], but high levels of FR are often over-expressed by epithelial cancer cells.[66 67] And this high level expression of FR by epithelial cancer cells provides an excellent mechanism for target-mediated (receptor-targeted) imaging and therapeutic.[73]

Since the discovery of an efficient delivery of folate-macromolecule conjugates via FR-mediated endocytosis[74], a varity of molecular functionalities have been successfully linked to FA to achieve FR-targeted delivery to tumor cells.[75 76 63 77] Other examples includes folate-conjugated dendrimers[78 79], anti-GFP siRNA that is delivered to

KB cells to achieve suppression of GFP expression[80] [81], folate-siRNA that delivers siRNA into KB cells[82], and folate-linked lipid nanoparticles.[83]

CHAPTER II

SIGNIFICANCE AND OBJECTIVES

Significance

Nowadays, most of the AuNP/siRNA delivery systems have positive-charged surfaces and are nonspecific. Similar to the positive lipoplexes and polyplexes discussed above, the cationic portrait would cause the rapid clearance from the circulation and significant toxicity because of membrane disruption, although it could also promote the uptake of nanoparticles. The nonspecific portrait, on the other hand, will result in the nonspecific binding of positively charged nanoparticles to the negatively charged cell membrane, which might induce nonspecific delivery of siRNA that will drastically reduce the therapeutic effect.

To overcome these problems, we propose to construct neutral and target-specific AuNP/siRNA nanoplexes as the delivery system, the structure of which is shown in Figure 6.

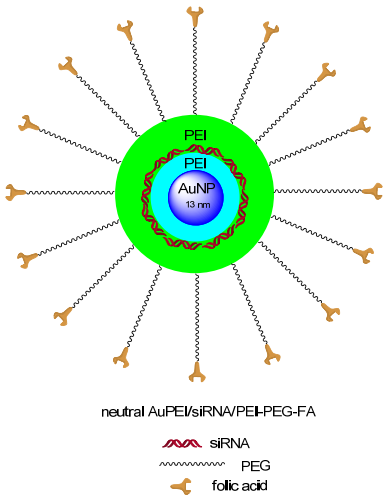

Figure 6. Structure of the proposed neutral AuPEI/siRNA/PEI-PEG-FA nanoplexes. AuNP = gold nanoparticles, PEI = polyethylenimine, PEG = polyethylene glycol, FA = folic acid

Hypotheses and Objectives

The hypotheses are summarized as follows:

1. The neutral character of the Au nanoplex will avoid the quick clearance and cytotoxicity that caused by the cationic nature of previous synthesized AuNP/siRNA complexes.

2. PEGylation will stabilize the nanoplexes in biological media and prolong their circulation time in blood stream so that the nanoplexes will have the sufficient time to accumulate in tumor due to the EPR effect.

3. Folic acid, served as the targeting group, would avoid the nonspecific delivery of siRNA, so the side effect caused by lack of tumor selectivity would be greatly reduced.

The basis of the first hypothesis comes from previous studies of stable nucleic acid lipid particle and functionalized PEIs. The reduced positive-charged liposome or polyplex have shown lower toxicity and surprisingly, in some cases, increased the transfection efficiency. The second hypothesis is based on the widely accepted fact that PEGlyation can increase the stability of different delivery systems (lipoplex, liposome, polyplex, and gold nanoparticles) and decrease the nonspecific interactions with serum protein and endothelium. The basis of the third hypothesis is that a variety of molecular functionalities have been successfully linked to FA to achieve FR-targeted delivery to tumor cells.

The objectives are summarized as follows:

1. Assembly of AuPEI/siRNA/PEI-PEG-FA through Layer-by-Layer approach.

2. Characterization of AuPEI/siRNA/PEI-PEG-FA by UV-vis spectrometry, DLS and zeta potential.

3. Evaluation of AuPEI/siRNA/PEI-PEG-FA in the FR+ cancer cell lines.

CHAPTER III

MATERIALS AND METHODS

Experimental Protocols

Synthesis of PEI-PEG-FA and PEI-PEG-mPEG Copolymers

109 mg of mPEG-SH (Polysciences) was dissolved in 1 mL of dry DMSO (Dimethyl sulfoxide, Fisher). To the mPEG-SH solution was added 70 ul of 318 mM MCNSP in dry DMSO. The rxn was stirred once in a while at r.t. for 2 h. 220 mg of 10k PEI (Polysciences) was dissolved in 600 ul in dry DMSO. Modified mPEG-MCNSP solution was added dropwise to PEI solution in 1: 1, 1: 2, and 1: 4 ratios. After 1 h, three conjugates were precipitated out by ether, re-dissolved in H_2O, and dialyzed by 3500 MW membrane. Then the three copolymers were transferred into the 45-mL tubes, frozen, lyophilized until dry, and stored at -20℃.

172 mg of FA-PEG-S-S-PEG-FA was dissolved in 3 mL of DMSO. 65 mg of DTT (Dithilthreitol) were dissolved in 1 mL of DMSO. Then DTT solution was added to the FA-PEG disulfide solution. The rxn was stirred at r.t. for 3 h. Then DTT was washed away by ether. Then the FA-PEG-SH was re-dissolved in dry DMSO, and added 98 ul of 318 mM MCNSP to the solution. The rxn was stirred once in a while at r.t. for 2 h. 318 mg of 10k bPEI was dissolved in 1206 ul DMSO. Modified FA-PEG-MCNSP solution was added dropwise to PEI solution in 1: 1, 1: 2, and 1: 4 ratios. After 1 h, three conjugates were precipitated out by ether, re-dissolved in H_2O, and dialyzed by 3500 MW membrane. Then the three copolymers were transferred into the 45-mL tubes, frozen, lyophilized until dry, and stored at -20℃.

In vitro Transcription of siGLuc-ppp and Tingle Strand RNA with 80 nt ($ssRNA_{80}$)

In vitro transcription of siGLuc. Mix 10 ul of 10X buffer (1X), 10 ul of 100 mM DTT (10 mM), 36 ul of 25 uM NTPs, 4 ul of DNA template, 1 ul of RNase inhibitor, and 10 ul of T7 polymerase in 30 ul of RNase-free water. The rxn mixture was incubated at 37℃ for 2 h. The crude siGLuc-ppp was obtained by ethanol precipitation and further purified by 8% PAGE gel to get pure siGLuc-ppp.

In vitro transcription of ssRNA80. 5 ul of Sigma water, 2 ul of 10X buffer (1X), 2 ul of 100 mM DTT (10 mM), 6 ul of 25 mM NTP (7.5 mM), 2 ul of DNA template (1 ul/10 ul rxn), and 1 ul of RNase inhibitor was added to 500-ul tube. After vortex, 2 ul of T7 RNA polymerase was added the mixture. The rxn was incubated at 37°C for 3 h. The crude $ssRNA_{80}$ was obtained by ethanol precipitation and further purified by 8% PAGE gel to get pure RNA molecules.

Layer-by-Layer Assembly of AuPEI/siRNA/PEI-PEG-FA

AuNP (13nm diameter) were synthesized by the reduction of chorloauric acid with a subsequent addition of citrate to precipitate gold ions into uncharged gold atoms, as previously described. Branched polyethylenimine (HS-$PEI_{1.8k}$ (1.8kDa) and HS-PEI_{10k} (10kDa)) was synthesized by conjugation of 11-mercaptoundecanoic acid (MUA) with PEI (Polysciences, Inc). HS-$PEI_{1.8k}$ was added to AuNPs at the final concentration of 0.5 mM, and the rxn was incubated at room temperature overnight. The thiol-modified AuNPs (AuPEI) were purified six times by centrifugation and re-suspended in aqueous solution. The purified AuPEI were added dropwise to the siRNA solution at room temperature overnight at a ratio of 500: 1 (siRNA: AuNPs). Excess siRNA was removed by 3x centrifugation (4.0 rcf, 80 min). The purified AuPEI/siRNA was added to the

solution of PEI-PEG-FA (or PEI, PEI-mPEG) at the ratio of 200: 1 (Polymer: AuPEI/siRNA). After 1x centrifugation (4.0 rcf, 20 min), the AuPEI/siRNA/PEI-PEI-FA was ready for the cellular study. After the deposition of each layer, the Au nanoplexes were characterized by UV-vis spectrometry, DLS (Dynamic light scattering), and zeta potential.

Enzymatic Degradation of AuPEI/siRNA/PEI

The purified AuPEI/si-3/PEI nanoplexes (300 pmol siRNA) were treated with Riboshredder RNase Blend (Epicenter Biotechnologies) (0.1 unit/500 ul RNase free Ultra-pure water), and the absorbance at 260 nm was minored using an Agilent 8453 UV-Visible spectrophotometer (Agilent Technologies) in "Kinetics" mode. The positive control, siRNA-3 only (si-3, 300 pmol) was also treated with Riboshredder RNase Blend at similar concentration. The spectrometer was blank with DNase/RNase Ultra pure water (Life Technologies), and the absorbance at 260 nm was monitored for 300s, with 60 data points acquired per minute.

Release of HS-PEI from AuPEI by DTT

HS-PEI-FITC was synthesized by the conjugation of FITC with HS-PEI. HS-PEI-FITC was added to AuNPs at the final concentration of 1.0 mM, and the rxn was incubated at room temperature overnight. The AuPEI-FITC were purified six times by centrifugation and re-suspended in aqueous solution. DTT was then added to the Au nanoplexes at various concentrations (100 mM, 200 mM, 500 mM, and 100 mM). The rxns were incubated at 70℃ for 1 h and centrifuged to remove the aggregates. The supernatant was measured by fluorescence spectroscopy, and the concentration of

released HS-PEI-FITC was calculated from the standard curve, which was prepared with a series of HS-PEI-FITC solution in the reaction condition.

Cell Culture

All the cell lines were maintained and proliferated in folate free RPMI 1640 cell media supplemented with 10% fetal calf serum (FCS), 100 units per ml penicillin, and 100 ug per ml streptomycin at 37 °C in 95% air humidified atmosphere, and 5% CO_2. Three of them (KB, SKOV3 and HeLa) express high levels of folate receptor while A549 cells express little. A KB-GLuc cell line that permanently expresses the Gaussia Luciferase is developed for the analysis of RNAi effects.

Downregulation of GLuc in KB-GLuc Cells by Au Nanoplexes

KB-GLuc cells were seeded in 48-well plates in folate free RPM1640 supplemented with 10% FBS 24 h before experiment. Dh/siGLuc-ppp was prepared following the standard protocol.[84] Then KB-GLuc cells were incubated with Dh/siGLuc-ppp and Au nanoplexes for 48 h, and the medium supernatant was analyzed by GLuc assay following the standard protocol.[84] The concentration of siGLuc-ppp was 100 nM.

Targeted Delivery of $ssRNA_{80}$ by Au Nanoplexes

KB-GLuc cells were seeded in 48-well plates in folate free RPM1640 supplemented with 10% FBS 24 h before experiment. Dh/$ssRNA_{80}$ was prepared following the standard protocol.[84] The KB-GLuc cells were incubated with Dh/$ssRNA_{80}$ and the Au nanoplexes for 2, 12 and 24 h in different culture media. Then all the media was switched to 10% FBS RPMI1640. After 48 h, the cell viability was analyzed by Toluidine blue (TB) assay.[84]

Downregulation of Luc in HeLa Cells by Au Nanoplexes

HeLa cells were seeded in 48-well plates in folate free RPM1640 supplemented with 10% FBS 24 h before experiment. Dh/pGL3 and Dh/siF17 was prepared following the standard protocol.[84] The KB-GLuc cells were first incubated with Dh/pGL3 for 1 h. After another 5 h, the KB-GLuc cells were further incubated with Dh/siF17 and Au nanoplexes for 6 h in different culture media. Then all the media was switched to 10% FBS RPMI1640. After 42 h, the cells were analyzed by Luc assay.[84]

CHAPTER IV

RESULTS

Layer-by-Layer Assembly of AuPEI/RNA/PEI-PEG-FA

To assemble the well-defined Au nanoplexes, the key is to avoid the aggregation caused by interparticle bridging. The aggregation not only lowers the yields but also makes their application in cell culture pointless. To develop the optimal procedure, each step in the assembly process should be carefully investigated.

Preparation of AuPEI

Figure 7 describes how the HS-PEI concentration in the reaction affected the hydrodynamic diameter, zeta potential, and size distribution of the purified AuPEI. When the [HS-PEI] was above 0.3 mM, the Au nanoplexes exhibited similar size (23.2 to 24.3 nm), zeta potential (55.2 to 56.0 mV), and size distribution. Once [HS-PEI] dropped to 0.1 mM, the aggregates of Au nanoplexes were formed, which increased the diameter of AuPEI to 45.8 nm and shifted the size distribution curve towards the large-size direction. Despite their large size, the aggregates still possessed the similar zeta potential as the rest of the Au nanoplexes.

Electrostatic repulsion is one major force that keeps the Au nanoplexes stable in the aqueous solution. To prevent forming aggregations, the nanoplexes should have enough surface charge to “push” other nanoplexes away. AuNPs are stabilized in solution by a high concentration (~ 0.3 mM) of citrate, a negatively charged molecule near pH 7. To overcome the charge and replace the citrate molecules completely, enough positive-charged HS-PEI should be added so that they can bind on the AuNPs and make them

stable in the solution. If the critical concentration of HS-PEI is not met (e.g. [HS-PEI] = 0.1 mM), aggregations will be formed during the assembly process.

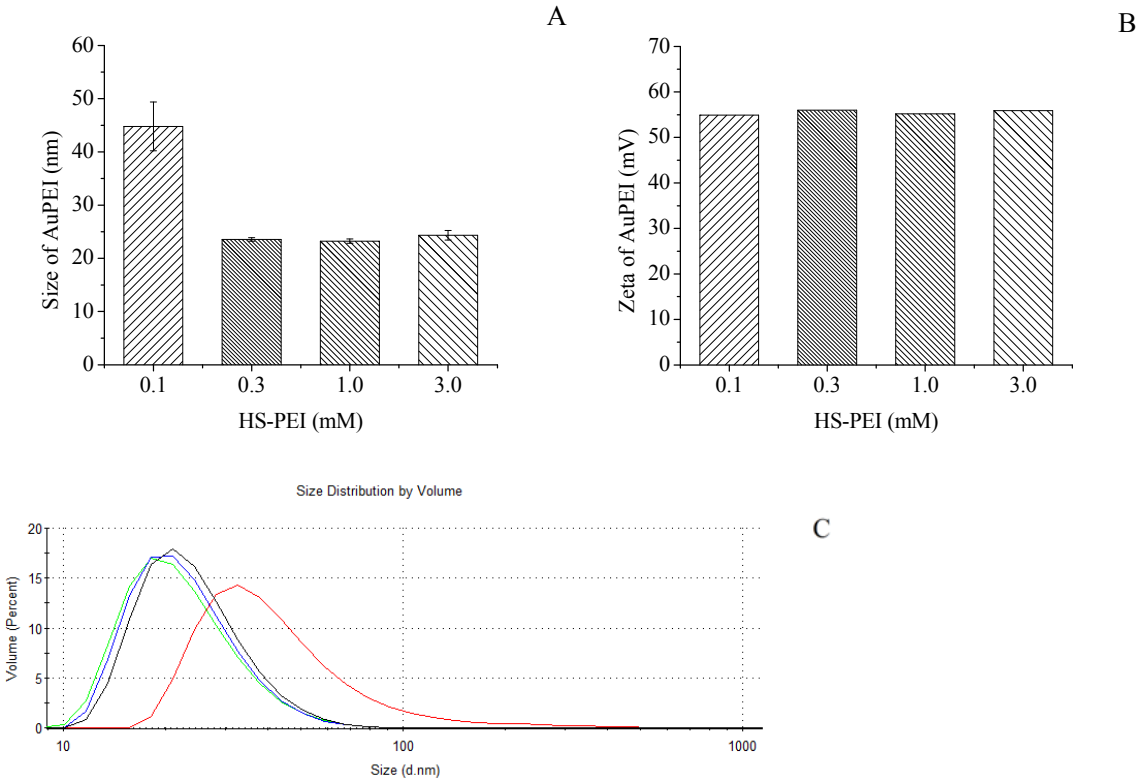

Figure 7. Characterization of AuPEI prepared in different HS-PEI solutions. (A) The effect of HS-PEI concentration on the hydrodynamic diameter of AuPEI after purification. (B) The corresponding zeta potential. (C) The corresponding size distribution: 0.1 mM (red), 0.3 mM (green), 1.0 mM (blue) and 3.0 mM (black). The error bar is standard deviation.

The Effect of Centrifugal Force on the Recovery of AuPEI/RNA

The major challenges in the assembly of the AuPEI/RRNA are the low recovery yield and the aggregation of the nanoplexes during purification. Centrifugal force and the ratio between AuPEI and RNA molecules are the two factors controlling that process. Using tRNA as the model molecule, Figure 8 describes how the centrifugal force affected the re-suspension of the AuPEI/tRNA after one centrifugation. It is clear that the absorbance of the re-suspended AuPEI/tRNA was increased as the centrifugal force

decreased, indicating the low rcf could greatly avoid the aggregation of AuPEI/tRNA during the purification process. The ratio effect is depicted in the next section.

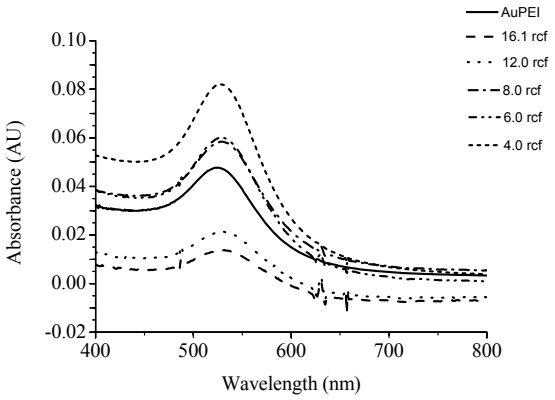

Figure 8. UV-vis spectra of the re-suspended AuPEI/tRNA (AuPEI/tRNA ratio was 1: 500) after 20 min centrifugation under different centrifugal force.

Preparation of AuPEI/RNA

To prepare aggregate-free AuPEI, the critical concentration should be reached. Similarly, to successfully coat RNA on the AuPEI, the critical ratio between AuPEI and RNA should be satisfied. The condition was investigated using tRNA as the model molecule. When mixing AuPEI and tRNA in ratio 1: 200, almost all the particles were precipitated out. Hence, the AuPEI/tRNA should be assembled in much higher tRNA/AuPEI ratio.

Figure 9 describes how the ratio of AuPEI: tRNA affected the hydrodynamic diameter, zeta potential, and size distribution of purified AuPEI/tRNA. When the ratio (1: 1000) was away from the critical ratio, the hydrodynamic diameter of AuPEI/tRNA was only 30.8 nm, and when the ratio (1: 400) was close to the critical ratio, the diameter (61.2 nm) was increased by two folds. Correspondingly, the size distribution of the AuPEI/tRNA had a right shift towards large-size direction. Although the aggregates were formed, the zeta potentials of the two species were still very close to -40 mV.

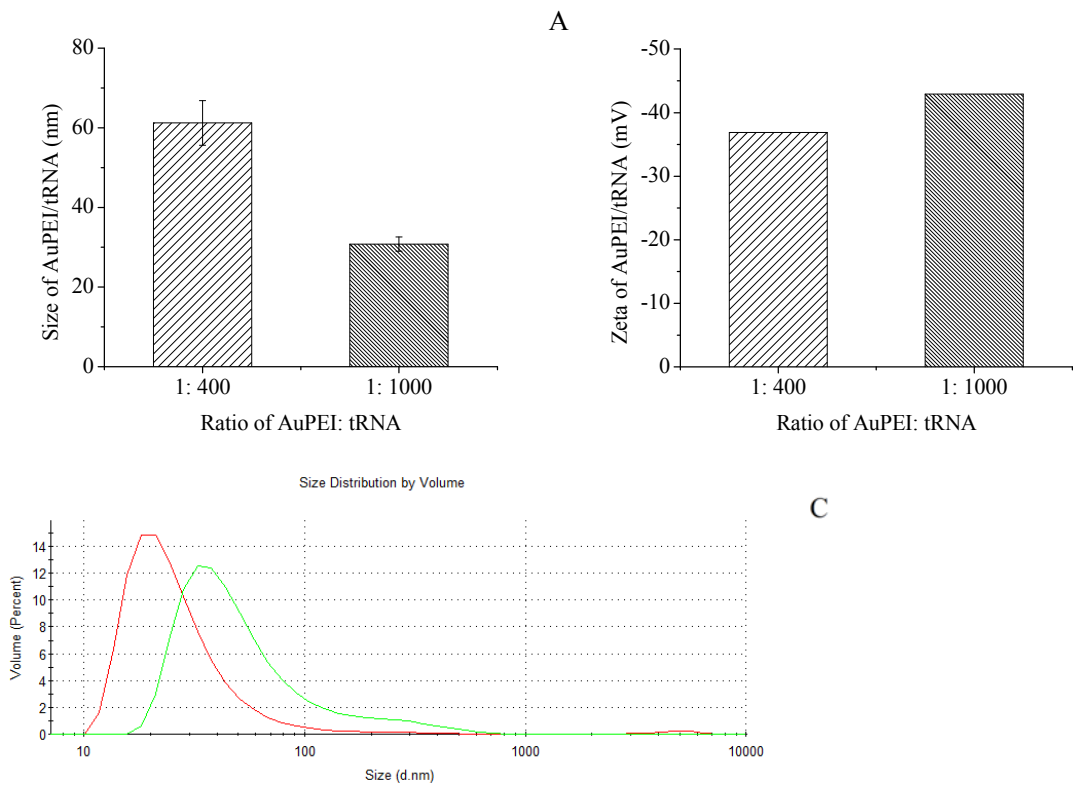

Figure 9. Characterization of AuPEI/tRNA prepared with different AuPEI: tRNA ratios. (A) The effect of AuPEI: tRNA ratio on the hydrodynamic diameter of AuPEI/tRNA after purification. (B) The corresponding zeta potential. (C) The corresponding size distribution: 1: 400 (green) and 1: 1000 (red). The error bar is standard deviation.

Preparation of AuPEI/tRNA/PEI-PEG

To assemble neutral AuPEI/RNA/PEI-PEG, AuPEI/tRNA and PEI-mPEG (PEG/PEI ratio was 2) were used to explore the conditions. Figure 10 describes the relationship between the zeta potential and the hydrodynamic diameter of the Au nanoplexes. When the ratio was 1: 50, the nanoplexes stayed in neutral (3.1 mV); however, its diameter reached 1303 nm, falling into micrometer range. When the ratio increased to 1: 250, the nanoplexes were positive charged (42.5 mV), and the diameter was only 61.4 nm. The distribution curve clearly showed the difference of the two nanoplexes in size.

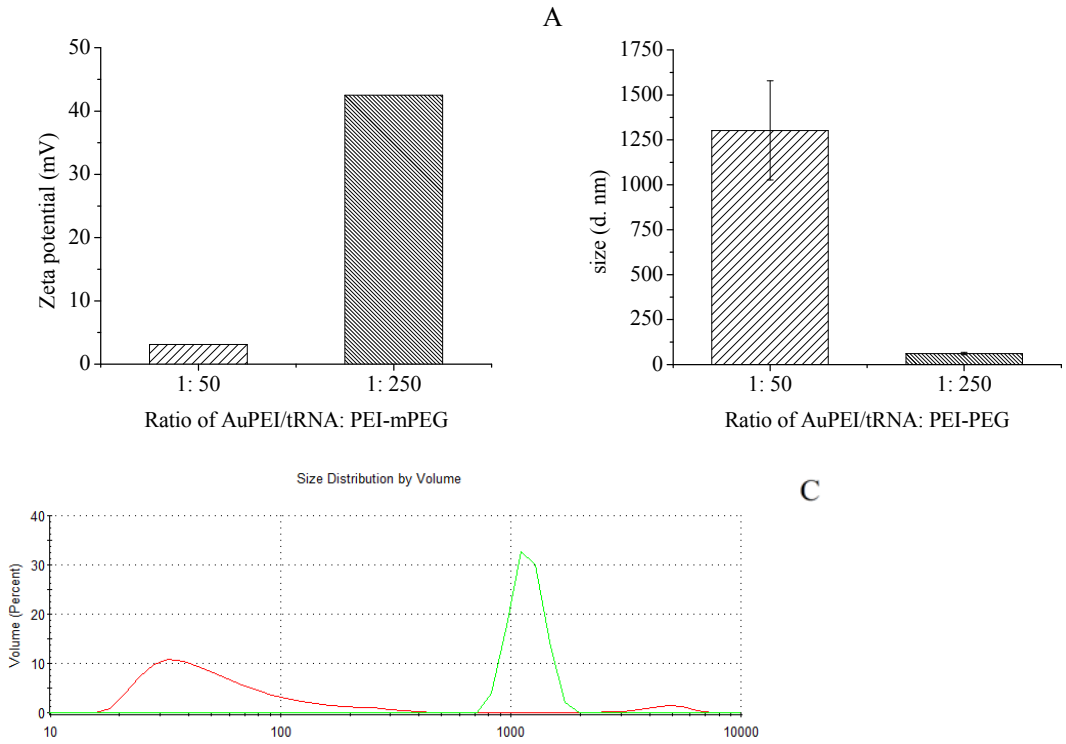

Figure 10. Characterization of AuPEI/tRNA/PEI-mPEG prepared with different AuPEI/tRNA: PEI-mPEG ratios. (A) The effect of AuPEI/tRNA: PEI-mPEG ratio on the zeta potential of AuPEI/tRNA/PEI-mPEG after purification. (B) The corresponding hydrodynamic diameter. (C) The corresponding size distribution: 1: 50 (green) and 1: 250 (red). The PEG/PEI ratio in the PEI-mPEG was 2. The error bar is standard deviation.

Then the other two PEI-mPEG copolymers were used as the third layer to assemble the AuPEI/tRNA/PEI-mPEG. Figure 11 describes how different PEI-mPEG copolymers affected hydrodynamic diameter and size distribution when all three species were neutral (Figure 11A). Although the higher PEG/PEI ratio resulted in a smaller hydrodynamic diameter and a left shift of the distribution curve, all the nanoplexes were too large for the siRNA delivery (Figure 11B-C), and their tendency of forming aggregates made them very unstable in the aqueous solution.

Clearly, the PEGylation cannot stabilize the neutral AuPEI/RNA/PEI-PEG in the aqueous solution, which also indicates that having enough charge on the surface of the Au nanoplexes is the key for them to "survive" in the solution.

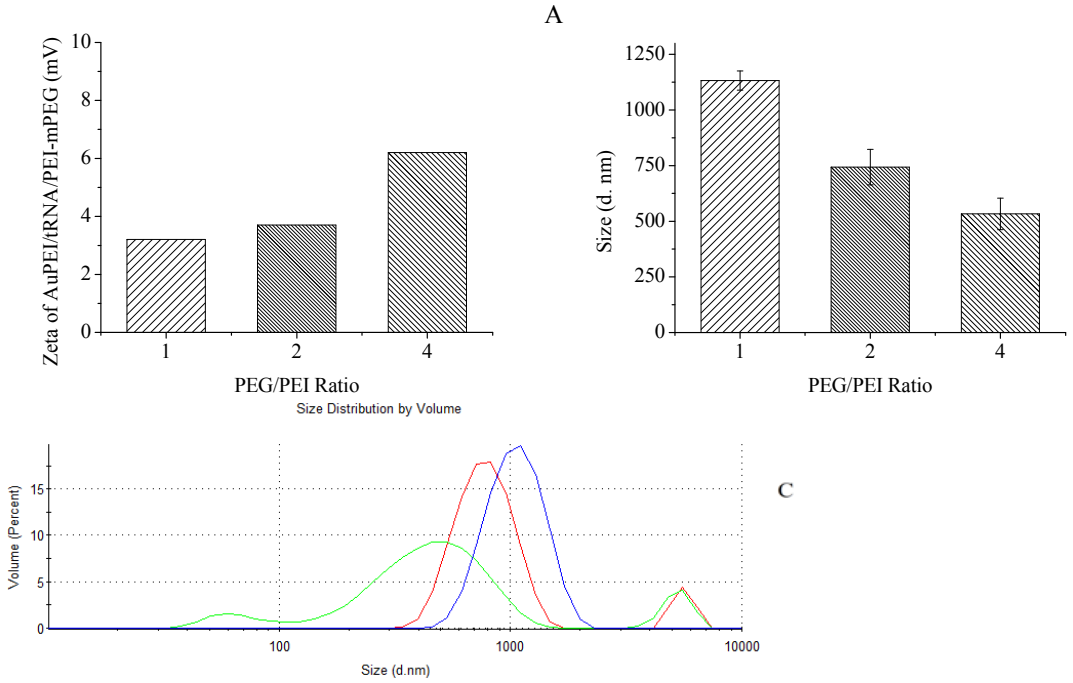

Figure 11. Characterization of AuPEI/tRNA/PEI-mPEG prepared with different PEI-mPEG. (A) The effect of PEG/PEI ratio on the zeta potential of AuPEI/tRNA/PEI-mPEG after purification. (B) The corresponding hydrodynamic diameter. (C) The corresponding size distribution: PEG/PEI=1 (blue), PEG/PEI=2 (red) and PEG/PEI=4 (green). The error bar is standard deviation.

Assembly of AuPEI/siRNA/PEI on Optimized Condition

Based on the above study, an optimized procedure was developed and applied for assembling stable AuPEI/siRNA/PEI, and the successful deposition of each layer was monitored by UV-vis spectra, DLS, and zeta potential measurements (shown in Figure 12A-D). Figure 11A details the increase of the hydrodynamic diameter of the Au nanoplexes during coating, which increased from 12.9 ± 0.3 nm (AuNPs) to 48.2 ± 3.7 nm (AuPEI/siRNA/PEI). The corresponding reversal of the zeta potential, shown in

Figure 12B, demonstrated the deposition of each layer. Figure 12C describes the UV-vis spectra of the Au nanoplexes. The maximum wavelength of the plasmon resonance peak, except the out PEI layer, had a red shift during coating. Additionally, the absorbance of AuPEI/siRNA/PEI in 220 – 320 nm UV-vis spectra proved the coating of the siRNA in the nanoplexes (Figure 12D).

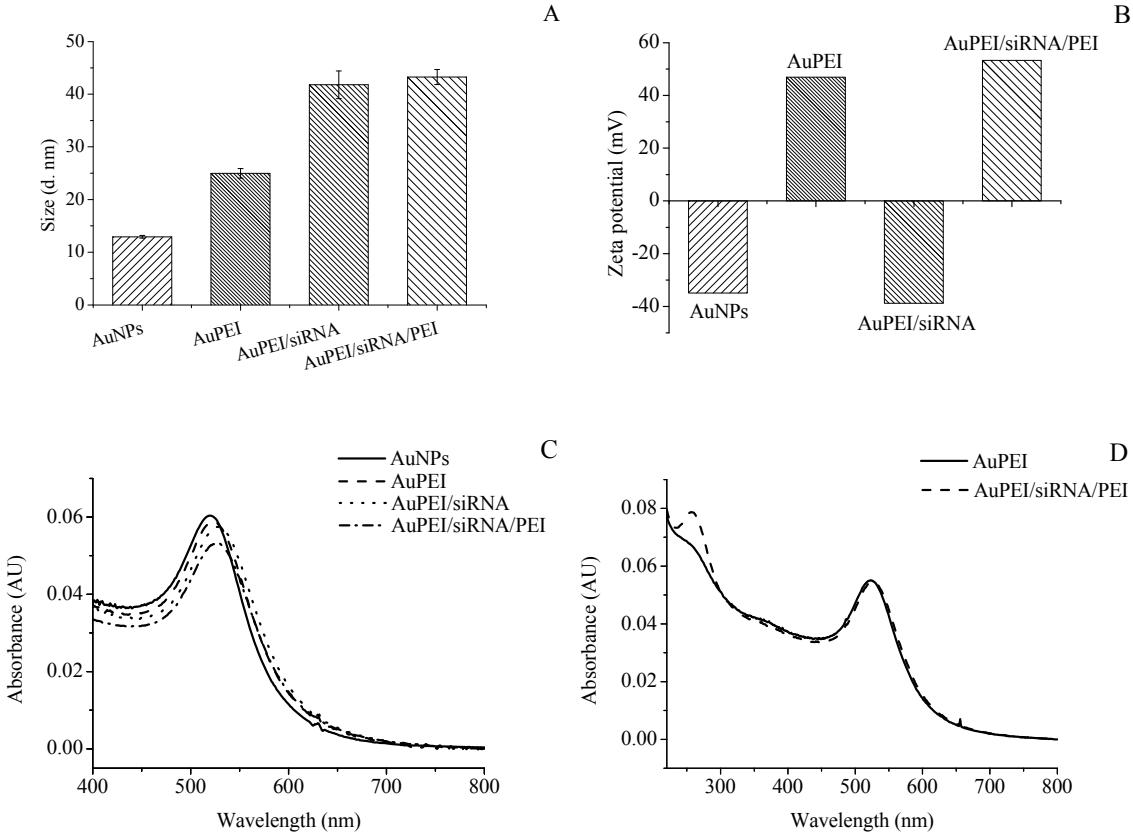

Figure 12. Characterization of Au nanoplexes during LbL assembly upon optimized conditions. (A) UV-vis spectra (400-800 nm) of AuNPs, AuPEI, AuPEI/siRNA and AuPEI/siRNA/PEI. (B) UV-vis spectra (220-800 nm) of AuPEI and AuPEI/siRNA/PEI. (C) Hydrodynamic diameter of the corresponding Au nanoplexes. (D) Zeta potential of the corresponding Au nanoplexes. The error bar is standard deviation.

Surface Density of the Layers in AuPEI/RNA/PEI-PEG-FA Nanoplex

Before applying the AuPEI/siRNA/PEI-PEG-FA to bio systems, it is better to know the number of RNA molecules that wrapped on the Au nanoplexes, or it is hard to control the concentration of siRNA in the cellular experiments.

Surface Density of the First Layer HS-PEI

To determine the surface density of HS-PEI, we used a strategy that is illustrated in Scheme 2. First, HS-PEI was labeled by FITC and coated on AuNPs following the optimized procedure. Then the fluorescent labeled AuPEI-FITC was treated with DTT solution in high concentrations. As a result, the HS-PEI-FITC molecules on the nanoplexes were replaced by DTT, released into the solution, and the DTT coated Au nanoparticles precipitated out from the solution. Finally, the released HS-PEI-FITC was quantified by fluorescence spectroscopy.

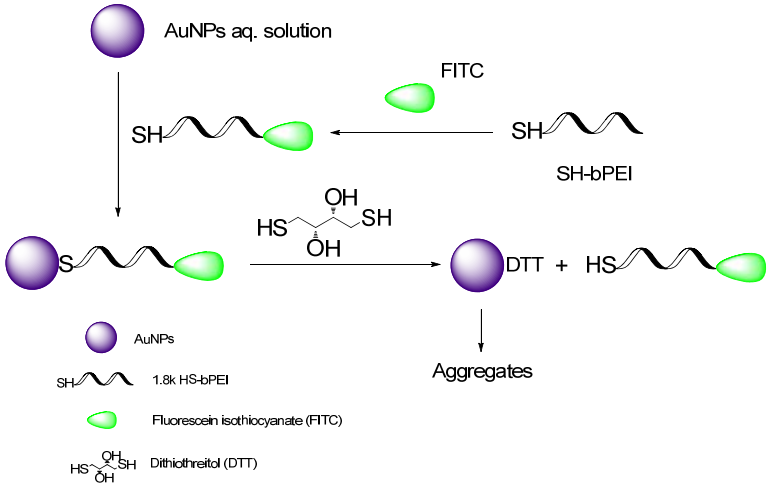

Figure 13. Flowchart illustrating the determination of surface density of HS-PEI on AuPEI.

Before determining the surface density of AuPEI-FITC, the standard curve of HS-PEI-FITC were prepared (Figure 14A, R-square = 0.996), and the effects of and temperature and DTT concentration (two major factors involved in the DTT replacement

reaction) on fluorescence signals were studied. Shown in Figure 14B, within in 60 min, the fluorescent counts of HS-PEI-FITC were relatively constant at various temperatures, indicating the fluorescent labeled HS-PEI molecules were stable in the aqueous solution even at high temperature. In DTT solution, due to the quenching effect, the fluorescent counts of HS-PEI-FITC were decreased over the DTT concentration, and such an effect reached to the maximum above 500 mM (Figure 14C). Within 200 mM, the decrease of the counts were in a linear relationship with the DTT concentration (Figure 14D, R-square = 0.998).

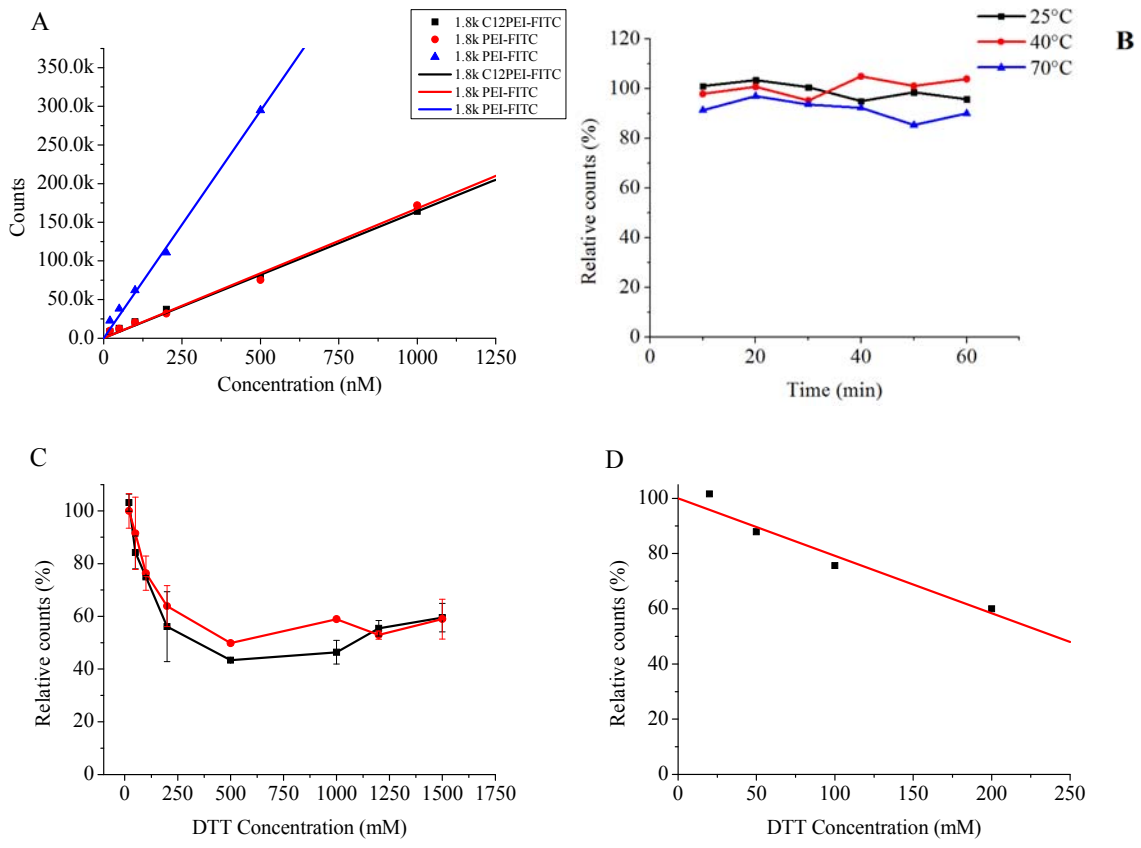

Figure 14. (A) Standard curve for quantification of the released HS-PEI-FITC from Au nanoplexes. (B) The effect of temperature on the fluorescence signals. (C-D) The effect of DTT concentration on the fluorescence signals. The error bar is standard deviation.

Since the temperature had little influence on the fluorescence signals, the DTT replacement reaction was conducted at 70℃. Figure 15 describes the kinetics of the release of HS-PEI-FITC under various DTT concentrations. In 100-200 mM range (Figure 15A), after 10 min, about 600 HS-PEI-FITC per Au nanoplex were replaced by DTT. After 30 min, about 900 HS-PEI-FITC per nanoplex were replaced. The large error bar in the 40 and 60 min made it hard to decide whether the curve reached to plateau or not. The replacement reaction was further conducted in 500 and 1000 mM DTT (Figure 15B). Despite the large error bar, the curve growth was decreased over the time, and after 60 min, such growth almost stopped. The kinetic study suggested all the HS-PEI-FITC were released from the AuPEI-FITC after 60 min incubation in 500 mM (or higher) DTT solution. The surface density of PEI on AuPEI was determined to be 1000 ± 100 per Au nanoplex.

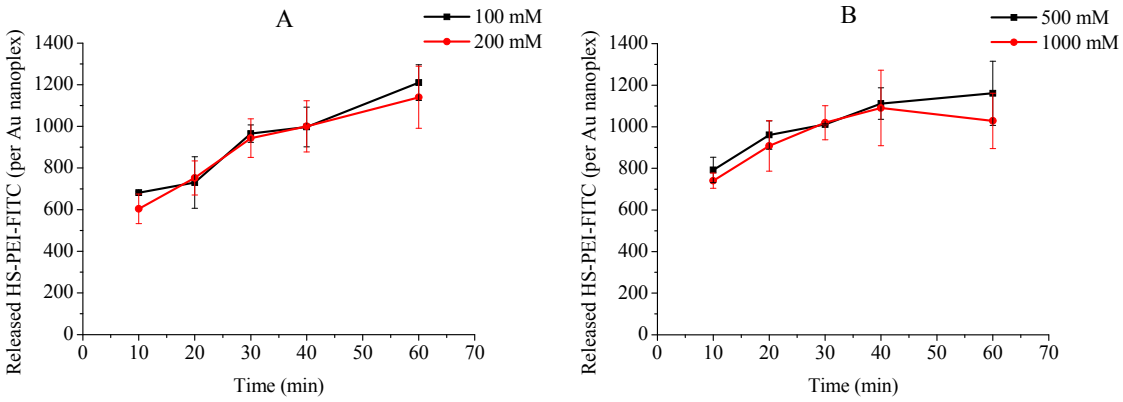

Figure 15. Release of HS-PEI-FITC from AuPEI-FITC by DTT after different incubation time. (A) Release of HS-PEI-FITC in 100 and 200 mM DTT. (B) Release of SH-PEI in 500 and 1000 mM DTT. The error bar is standard deviation.

Surface Density of RNA Layer

To determine the surface density of the RNA molecules, we applied a strategy reported in the literature.[55] The amount of the RNA wrapped around the AuPEI was

calculated from the formula (amount of RNA added - amount of RNA removed during purification).[55] The concentration of the purified AuPEI/RNA was determined by UV-vis, so their amount can also be calculated. The surface density of RNA equals the amount of coated RNAs over the amount of Au nanoplexes.

Different RNAs (tRNA, siGLuc, and siRNA (antivirus)) were coated on AuPEI, and their surface densities were calculated respectively (Figure 16). The results suggested that the surface density was co-related with the nucleotide length of the RNA molecule. AuPEI/tRNA (80 nt) has 150 tRNA per Au nanoplex while AuPEI/siGLuc (60 nt) had ~200. On AuPEI/siRNA (antivirus, 40 nt), the number was increased to ~290 per Au nanoplex.

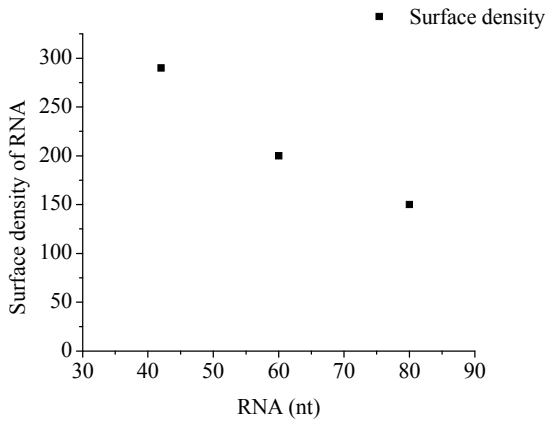

Figure 16. The surface density of antivirus RNA (42 nt), siGLuc (60 nt) and tRNA (80 nt) on AuPEI/RNA.

Protection of siRNA from RNase Degradation

Figure 17 showed the protection of siRNA from AuPEI/si-3/PEI in RNase enzymes solution. The naked si-3 was used as a control, which exhibited an increase in the absorbance at 260 nm (%) after RNase Riboshedder was added to the solution, suggesting degradation of naked si-3. In contrast, the AuPEI/si-3/PEI samples treated

with the RNase enzyme did not increase absorbance (%), indicating that the siRNA in the nanoplexes remained intact.

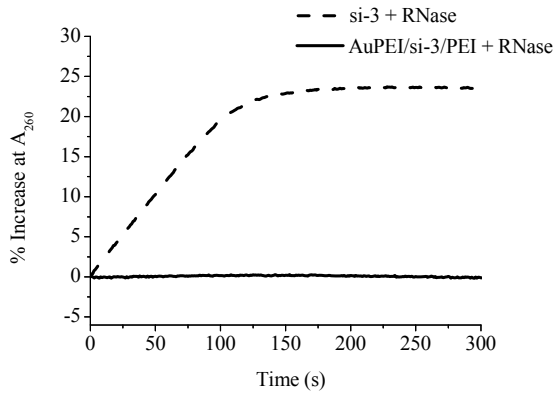

Figure 17. Absorbance at 260 nm (%) of si-3 and AuPEI/si-3/PEI in RNase solution.

Stability of Au Nanoplexes in Different Cell Culture Medium

The stability of Au nanoplexes in biological fluids is a requisite for their application in the cell culture. AuPEI/tRNA/PEI-mPEG with various AuPEI/tRNA: PEI-mPEG ratios (1: 10, 1: 200 and 1: 500) were assembled, applied to different biological media, and their behaviors were monitored by UV-vis spectroscopy.

All the nanoplexes can be divided into two groups based on their surface charge. AuPEI/tRNA and AuPEI/tRNA/PEI-mPEG (1: 10) were negatively charged, and AuPEI/tRNA/PEI-mPEG (1: 200) and AuPEI/tRNA/PEI-mPEG (1: 500) were positively charged. In serum-free RPMI solution, the negative-charged Au nanoplexes aggregated after 1 h incubation (Figure 18A-B) while almost half positive-charged species still remained disaggregated (Figure 18C-D). In the serum containing RPMI solution, the negative charged nanoplexes still aggregated, but the addition of FBS slowed down the aggregation process, especially in 40% FBS RPMI (Figure 18A-B). The positive-charged nanoplexes exhibited good stabilities in the FBS containing medium (Figure 18C-D).

Hence, the positive-charged Au nanoplexes were qualified candidates for the cellular study.

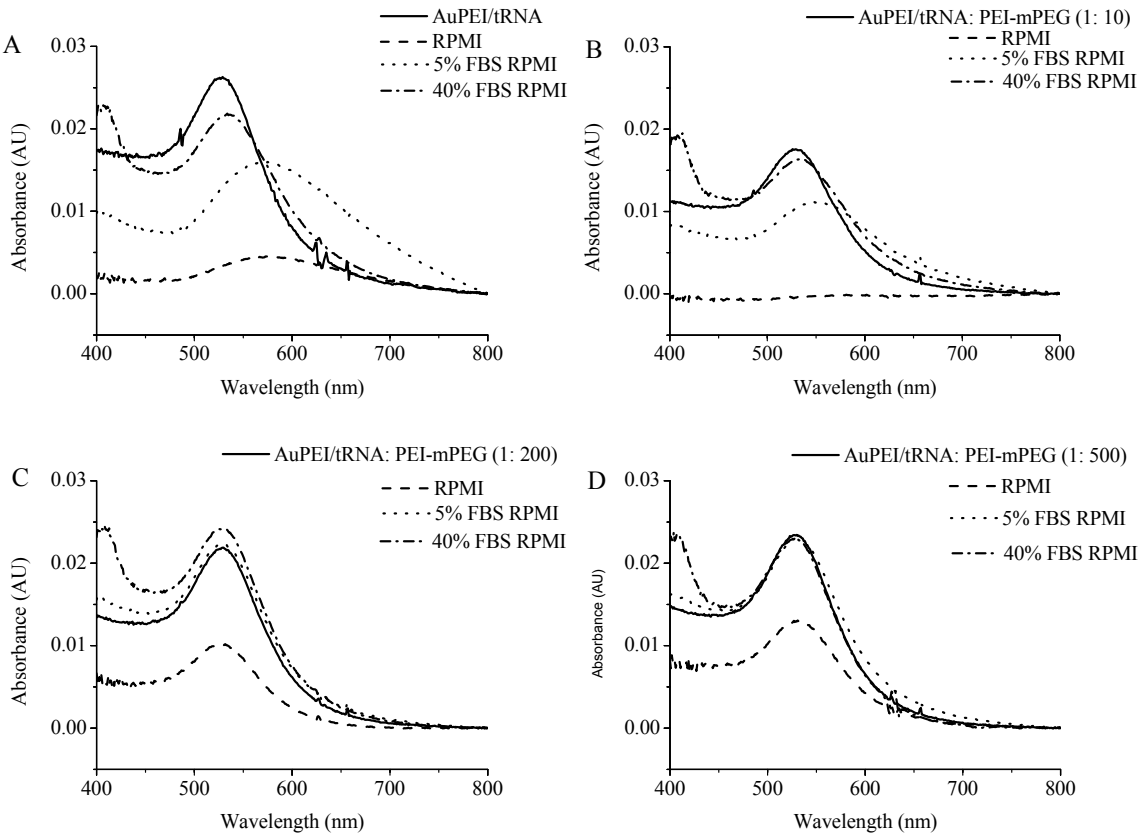

Figure 18. UV-vis spectra of Au nanoplexes in different media (serum free RPMI, 5% FBS RPMI and 40% FBS RPMI). (A) The UV-vis spectra of AuPEI/tRNA. (B) The UV-vis spectra of AuPEI/tRNA/PEI-mPEG (1: 10). (C) The UV-vis spectra of AuPEI/tRNA/PEI-mPEG (1: 200). (D) The UV-vis spectra of AuPEI/tRNA/PEI-mPEG (1: 500). The Au nanoplexes were incubated in the medium for 1 h and monitored by UV-vis spectrometry.

After exposed to the 5% FBS RPMI, the AuPEI/tRNA/PEI-mPEG (1: 200) was characterized by DLS and zeta potential measurements (shown in Figure 19). The size of the nanoplexes increased from 48.2 ± 3.7 nm to 78.8 ± 3.4 nm, and the zeta potential became near neutral (slightly negatively charged).

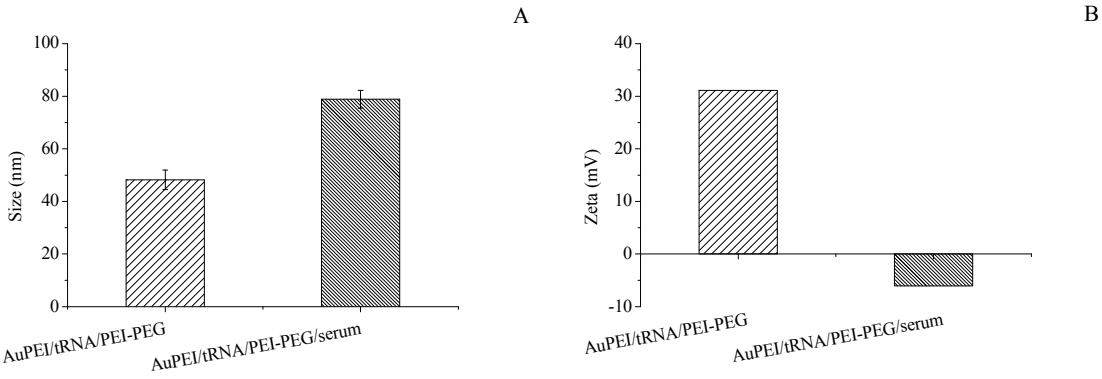

Figure 19. Hydrodynamic diameter (A) and zeta potential (B) of AuPEI/tRNA/PEI-mPEG in 5% FBS RPMI. The Au nanoplexes were prepared in 1: 200 AuPEI/tRNA: PEI-mPEG ratio.

Targeted Delivery of RNA by AuPEI/RNA/PEI-PEG-FA

Targeted Delivery of siGLuc and Downregulation of Gaussia Luciferase in KB-GLuc Cells

siGLuc-ppp was synthesized via in vitro transcription and incorporated into the Au nanoplexes following the optimized procedure. Using the DharmaFECT as the positive control, siGLuc-ppp was delivered into KB-GLuc cells by the designed Au nanoplexes. The expression of GLuc was monitored by GLuc assay to quantify the delivery efficiency (Figure 20A). After 48 h, the gene silencing efficiency was ~ 60% for Dh/siGLuc-ppp and was none for both AuPEI and AuPEI/siGLuc-ppp. However, no apparent difference was observed between nanoplexes AuPEI/siGLuc-ppp/PEI-mPEG (no gene silencing) and AuPEI/siGLuc-ppp/PEI-PEG-FA (~ 7%) in the presence of 8% serum. AuPEI/siGLuc-ppp alone did not show any gene silencing, but when mixed with DharmaFECT, the efficiency increased to ~86% (Figure 20C). The cell viability was monitored by TB assay (Figure 20B). Dh/siGLuc leaded to 40% decrease in cell number, but all the Au nanoplexes showed no cytotoxicity.

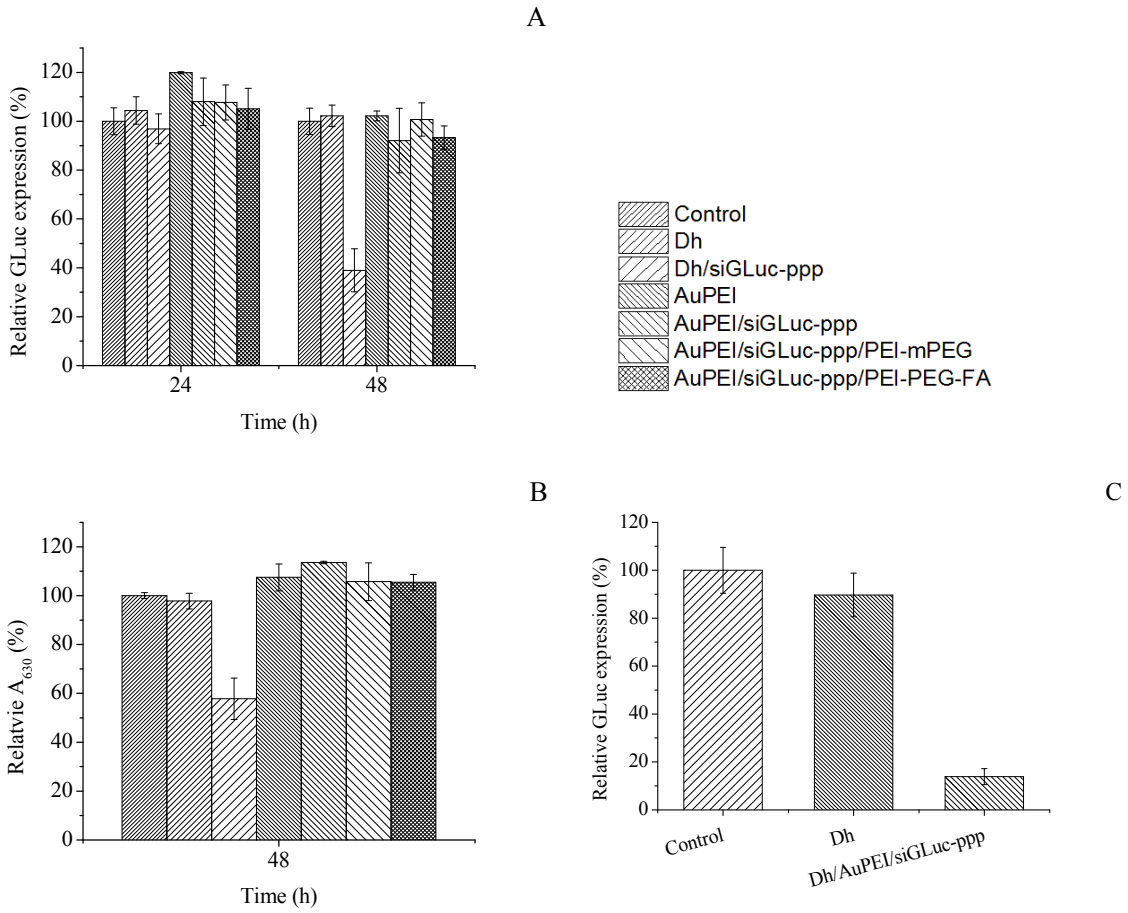

Figure 20. Targeted delivery of siGLuc into KB-GLuc cells. (A) Downregulation of GLuc in KB-GLuc cells by Au-based siGLuc-ppp nanoplexes. The [siGLuc-ppp] was 100 nM. After 24 h or 48 h, 10 ul of the culture supernatant was analyzed by GLuc assay. (B) Cell viability of the corresponding Au nanoplexes. After 48 h (including the incubation time), the cells were washed, fixed and stained with Toluidine Blue. Then the cells were washed with 2% SDS solution, of which the absorbance at 630 nm was measured. (C) Downregulation of GLuc in KB-GLuc cells by the mixture of DharmaFECT and AuPEI/siGLuc-ppp. After 48 h, 10 ul of the culture supernatant was analyzed by GLuc assay. The error bar is standard deviation.

Targeted Delivery of ssRNA$_{80}$ in KB-GLuc Cells in Different Cell Media

ssRNA$_{80}$ was demonstrated to have had strong cellular toxicity in cancer cells. To confirm the result from GLuc downregulation study, ssRNA$_{80}$ was synthesized and assembled into Au nanoplexes following the optimized procedure. After transfection into KB-GLuc cells, the cell viability was monitored by TB assay to quantify the delivery

efficiency. Figure 21A describes the cytotoxicity of AuPEI/ssRNA/PEI in various media. In 8% serum medium and Opti-MEM, AuPEI/ssRNA/PEI exhibited no delivery of ssRNA while in the serum-free medium, the cell number was decreased by ~ 53%. Figure 21B describes how the outer layer of Au nanoplexes in serum-free medium affected the cell viability. After 2 h incubation with AuPEI/ssRNA/PEI, the cytotoxicity in KB-GLuc cells reached ~ 60%. AuPEI/ssRNA/PEI-mPEG showed no toxicity at all. For cells treated with AuPEI/ssRNA/PEI-mPEG-FA, the toxicity was near ~ 20%.

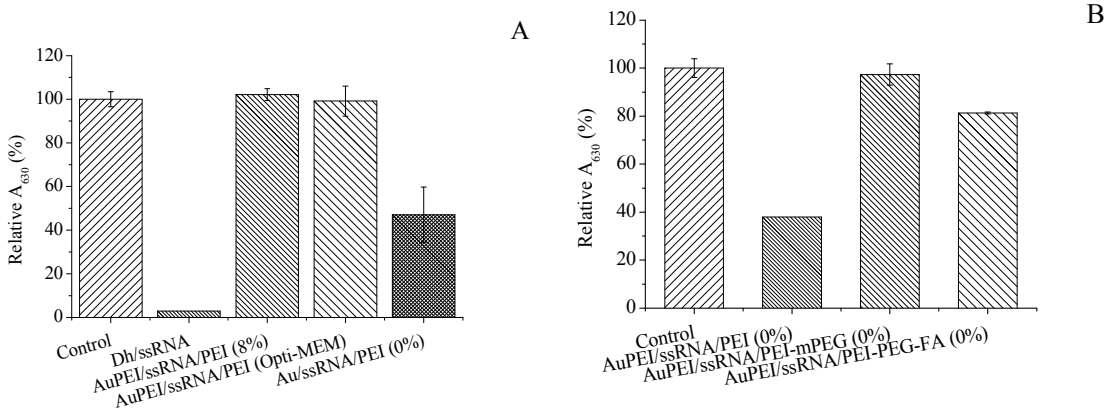

Figure 21. Delivery of $ssRNA_{80}$ (100 nM) into KB-GLuc cells by AuPEI/ssRNA/PEI. KB-GLuc cells were used as the control. The percentage in the figure represents the serum concentration in the cell culture. Incubation time represents how long the cells were incubated with Au nanoplexes. After 72 h (including the incubation time), the cells were washed, fixed and stained with TB. Then the cells were washed with 2% SDS solution, of which the absorbance at 630 nm was measured. The error bar is standard deviation.

Targeted Delivery of siF17 into HeLa cells and Downregulation of Luciferase Expression

To further confirm the results from above, the targeted delivery of our Au nanoplexes were investigated in HeLa cell line. Figure 23A describes gene silencing of Luciferase of AuPEI/siF17/PEI in various media. After 42 h, the gene silencing efficiency was ~ 9% for the AuPEI/siF17/PEI in the presence of 8% serum, ~ 41% in the 2% serum and ~ 76% in 0% serum. The gene silencing efficiency was greatly increased

as the serum was removed from the medium. Figure 23B describes the gene silencing efficiency of AuPEI/siF17/PEI-mPEG and AuPEI/siF17/PEI-PEG-FA in 8% and 0% serum media. Although the AuPEI/siF17/PEI-mPEG exhibited no gene silencing in both media, no apparent difference was observed between the none-FA nanoplexes and the FA modified nanoplexes.

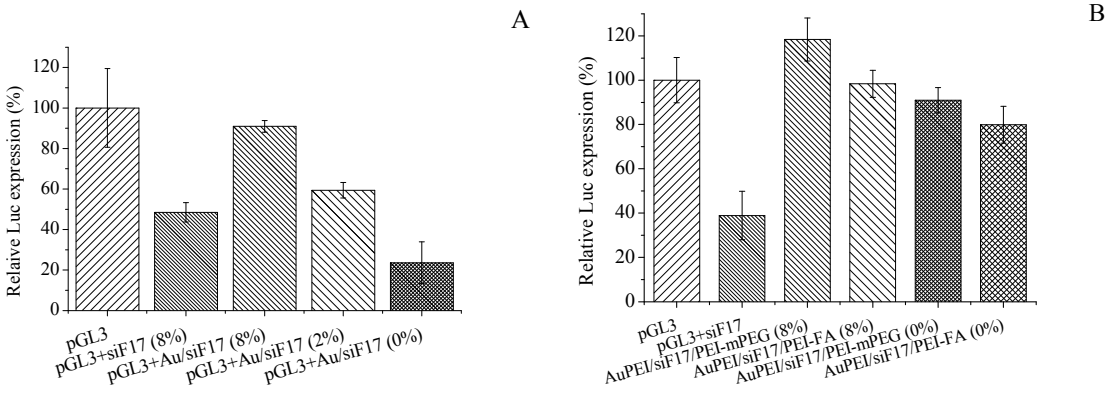

Figure 22. (A) Downregulation of Luc in HeLa cells by AuPEI/siF17/PEI in different cell media. (B) Downregulation of Luc in HeLa cells by AuPEI/siF17/PEI-PEG-FA in different cell media. HeLa cells were used as the control. The [siF17] was 100 nM. The percentage in the figure represents the serum concentration in the cell culture. After 42 h, the cells were lysed and the extracts were analyzed by Luc assay. The error bar is standard deviation.

The results of the RNA delivery by Au nanoplexes in the KB-GLuc and HeLa cell lines indicated that the delivery by AuPEI/RNA/PEI was greatly dependent on the serum content in the medium. They also suggested that PEGylation can perfectly prevent the nonspecific delivery by AuPEI/RNA/PEI. The targeted delivery of RNA by AuPEI/RNA/PEI-PEG-FA remained doubtful and needs further exploration.

CHAPTER V

SUMMARY AND FUTURE DIRECTION

Major Findings and Significance

To assemble well-defined and disaggregated Au nanoplexes through Layer-by-Layer approach, there existed the critical concentration for the deposited macromolecules or critical ratio of the Au nanoplex: deposited macromolecules. If the requirement is not stratified, the Au nanoplex tends to form aggregates.

High centrifugal force caused flocculation and a low recovery yield during the purification process of the Au nanoplexes, especially when the electrostatic interaction was the main force between the two layers. Purified under the optimized condition, the recovery yield can reach near 90%, and the interparticle bridging and the flocculation can be completely avoided.

A well-defined and mono-dispersed Au nanoplexes AuPEI/siRNA/PEI has been successfully assembled and well characterized. The nanoplex had a hydrodynamic diameter of 48.2 ± 3.7 nm and zeta potential of 53.3 mV. The surface density of the first layer HS-PEI was ~ 1000 per particle. Versatility is one important advantage of the developed nanoplexes. The siRNA middle layer can be expanded to any other RNA molecules, even DNA molecules and the surface density depended on its nucleotide length. Since the AuPEI had certain binding capacity, which came from the amine groups on branched PEI, shorter RNA (or DNA) molecules tended to have a higher surface density while longer ones bound less.

Our optimized Au nanoplexes can stabilize siRNA molecules and protect them from RNase degradation. The reason is straightforward: siRNA molecules were in the

middle of the two PEI layers, which acted as "walls" to inhibit the interaction of RNase with the siRNA molecules.

Our optimized Au nanoplexes were stable in the in vitro cell culture medium in presence of the serum, which provides the ground for their application in the in vitro study.

In terms of siRNA delivery, the Au nanoplexes AuPEI/siRNA/PEI exhibited excellent gene silencing efficiency in the absence of the serum during the transfection. The serum in the medium stabilized the Au nanoplexes but also made the siRNA delivery much less effective. Because the nanoplexes were positively charged, its strong interaction with the serum protein prevented its further contact with the cell membrane, so the delivery efficiency was greatly reduced.

In term of targeted delivery, PEGylation greatly reduced the nonspecific delivery of siRNA caused by AuPEI/siRNA/PEI. With PEGylation, AuPEI/RNA/PEI-mPEG showed almost no cytotoxicity (when RNA is $ssRNA_{80}$) or no knockdown of the targeted gene (when RNA is siGLuc-ppp or siF17). According to these results, their applications in the targeted delivery became possible.

Major Issues and Discussions

1. Neutral Au nanoplexes AuPEI/RNA/PEI-PEG are not stable in the aqueous solution, not mentioning in the cell culture medium. The PEI-PEG copolymers (PEG/PEI ratios are 1, 2, and 4) we applied here cannot provide enough repulsive force against the hydrophobic interactions between the neutral nanoplexes. Low surface density of the PEG on the neutral nanoplexes is the reason. Au nanoparticles with complete PEG coating by covalent bond have been synthesized and studied both in vitro[85] and in vivo.[86]

One strategy to the issue is to raise the PEG/PEI ratio, but it will reduce the positive charges on the PEI and affect the binding between AuPEI/RNA and PEI-PEG.

2. The major issue is that even though the AuPEI/ssRNA$_{80}$/PEI-PEG-FA caused more cell death than its PEI-mPEG counterpart, Au nanoplexes AuPEI/siRNA/PEI-PEG-FA (siRNA = siGLuc-ppp and siF17) showed no gene knockdown efficiency in the presence nor absence of the serum during the transfection.

Strength of the receptor-ligand interactions, ligand density, the length as well as rigidity of the spacer between the target molecule and anchor can strongly affect the final equilibrium of receptor-mediated endocytosis.[87] [65] The cellular uptake could also be mediated by the displacement of serum proteins by the receptors.[88] High binding affinity ($K_d \sim 10^{-10}$ M) of folic acid for the folate receptor indicated the existence of strong FR receptor-folic acid interaction.[89] The failed delivery of siRNA by AuPEI/siRNA/PEI in the presence of serum protein indicated its strong interactions with the serum proteins. Such binding is so strong that the coated proteins are difficult to be replaced, exposing the naked nanoparticles to the cell membrane. This also explains why no delivery took place from AuPEI/siRNA/PEI-mPEG and AuPEI/siRNA/PEI-PEG-FA in the serum-containing medium. In the serum-free medium, although AuPEI/siRNA/PEI showed satisfied delivery efficiency and PEGylation inhibited the nonspecific delivery, targeted delivery by AuPEI/siRNA/PEI-PEG-FA still remained unclear.

To figure this out, 1) the surface density of FA on the Au nanoplexes should be known. For liposomes, a mole fraction of 0.03-0.5% folate-PEG was found to be optimal for effective delivery.[65] The existence of optimal folate-PEG is probably true for the Au nanoplexes, too. Without knowing such information, any improvement is hard to be made.

2) The length of the PEG spacer also needs to be explored. Having shorter PEG chain (e.g., PEG_{2000}) in the targeted liposomes achieved better tumor targeting than PEG_{3400} and PEG_{5000}.[65] 3) Connecting FA to AuNPs through covalent linkage is proved to be an efficient approach to achieve targeted delivery.[90 91 92] Hence, conjugating PEG-FA on our Au nanoplexes through Au-S covalent bond is worthy of investigation.

Future Directions

Fast fabrication, versatility, and ability for siRNA protection are the major characters of our newly developed Au nanoplex system. The high gene silencing efficiency in the absence of serum makes it an excellent delivery agent for negative-charged macromolecules *in vitro*. The low gene silencing efficiency in the presence of serum hinders its application *in vivo*. How to reduce its strong interaction with serum without sacrificing its stability in the culture medium is one of the future directions. The application of the system in targeted delivery needs more exploration: the surface density of the FA, the effect of PEG spacer, and the conjugation manner of PEG-FA, which are definitely other interesting directions to pursue.

REFERENCES

1. American Cancer Society. Cancer Facts & Figures 2013. Atlanta: American Cancer Society; **2013**.

2. DeVita, V. T., Jr.; Chu, E., A history of cancer chemotherapy. *Cancer research* **2008,** *68* (21), 8643-53.

3. Fang, J.; Nakamura, H.; Maeda, H., The EPR effect: Unique features of tumor blood vessels for drug delivery, factors involved, and limitations and augmentation of the effect. *Advanced drug delivery reviews* **2011,** *63* (3), 136-51.

4. Raguz, S.; Yague, E., Resistance to chemotherapy: new treatments and novel insights into an old problem. *British journal of cancer* **2008,** *99* (3), 387-91.

5. Goodman, L. S.; Wintrobe, M. M.; et al., Nitrogen mustard therapy; use of methyl-bis (beta-chloroethyl) amine hydrochloride and tris (beta-chloroethyl) amine hydrochloride for Hodgkin's disease, lymphosarcoma, leukemia and certain allied and miscellaneous disorders. *Journal of the American Medical Association* **1946,** *132*, 126-32.

6. Gottesman, M. M., Mechanisms of cancer drug resistance. *Annual review of medicine* **2002,** *53*, 615-27.

7. Goldstein, L. J.; Galski, H.; Fojo, A.; Willingham, M.; Lai, S. L.; Gazdar, A.; Pirker, R.; Green, A.; Crist, W.; Brodeur, G. M.; et al., Expression of a multidrug resistance gene in human cancers. *Journal of the National Cancer Institute* **1989,** *81* (2), 116-24.

8. Bogman, K.; Peyer, A. K.; Torok, M.; Kusters, E.; Drewe, J., HMG-CoA reductase inhibitors and P-glycoprotein modulation. *British journal of pharmacology* **2001,** *132* (6), 1183-92.

9. Ramachandra, M.; Ambudkar, S. V.; Chen, D.; Hrycyna, C. A.; Dey, S.; Gottesman, M. M.; Pastan, I., Human P-glycoprotein exhibits reduced affinity for substrates during a catalytic transition state. *Biochemistry* **1998,** *37* (14), 5010-9.

10. Elbashir, S. M.; Harborth, J.; Lendeckel, W.; Yalcin, A.; Weber, K.; Tuschl, T., Duplexes of 21-nucleotide RNAs mediate RNA interference in cultured mammalian cells. *Nature* **2001,** *411* (6836), 494-8.

11. McCaffrey, A. P.; Meuse, L.; Pham, T. T.; Conklin, D. S.; Hannon, G. J.; Kay, M. A., RNA interference in adult mice. *Nature* **2002,** *418* (6893), 38-9.

12. Whitehead, K. A.; Langer, R.; Anderson, D. G., Knocking down barriers: advances in siRNA delivery. *Nature reviews. Drug discovery* **2009,** *8* (2), 129-38.

13. Petrocca, F.; Lieberman, J., Promise and challenge of RNA interference-based therapy for cancer. *Journal of clinical oncology : official journal of the American Society of Clinical Oncology* **2011,** *29* (6), 747-54.

14. Gartel, A. L.; Kandel, E. S., RNA interference in cancer. *Biomolecular engineering* **2006,** *23* (1), 17-34.

15. van de Water, F. M.; Boerman, O. C.; Wouterse, A. C.; Peters, J. G.; Russel, F. G.; Masereeuw, R., Intravenously administered short interfering RNA accumulates in the kidney and selectively suppresses gene function in renal proximal tubules. *Drug metabolism and disposition: the biological fate of chemicals* **2006,** *34* (8), 1393-7.

16. Castanotto, D.; Rossi, J. J., The promises and pitfalls of RNA-interference-based therapeutics. *Nature* **2009,** *457* (7228), 426-33.

17. Choi, C. H.; Alabi, C. A.; Webster, P.; Davis, M. E., Mechanism of active targeting in solid tumors with transferrin-containing gold nanoparticles. *Proceedings of the National Academy of Sciences of the United States of America* **2010,** *107* (3), 1235-40.

18. Wang, J.; Lu, Z.; Wientjes, M. G.; Au, J. L., Delivery of siRNA therapeutics: barriers and carriers. *The AAPS journal* **2010,** *12* (4), 492-503.

19. Jain, R. K., Transport of molecules in the tumor interstitium: a review. *Cancer research* **1987,** *47* (12), 3039-51.

20. Goula, D.; Becker, N.; Lemkine, G. F.; Normandie, P.; Rodrigues, J.; Mantero, S.; Levi, G.; Demeneix, B. A., Rapid crossing of the pulmonary endothelial barrier by polyethylenimine/DNA complexes. *Gene therapy* **2000,** *7* (6), 499-504.

21. (a) Mukherjee, S.; Ghosh, R. N.; Maxfield, F. R., Endocytosis. *Physiological reviews* **1997,** *77* (3), 759-803; (b) Endoh, T.; Ohtsuki, T., Cellular siRNA delivery using cell-penetrating peptides modified for endosomal escape. *Advanced drug delivery reviews* **2009,** *61* (9), 704-9; (c) Tseng, Y. C.; Mozumdar, S.; Huang, L., Lipid-based systemic delivery of siRNA. *Advanced drug delivery reviews* **2009,** *61* (9), 721-31.

22. Brummelkamp, T. R.; Bernards, R.; Agami, R., A system for stable expression of short interfering RNAs in mammalian cells. *Science* **2002,** *296* (5567), 550-3.

23. Pack, D. W.; Hoffman, A. S.; Pun, S.; Stayton, P. S., Design and development of polymers for gene delivery. *Nature reviews. Drug discovery* **2005,** *4* (7), 581-93.

24. Mintzer, M. A.; Simanek, E. E., Nonviral vectors for gene delivery. *Chemical reviews* **2009,** *109* (2), 259-302.

25. Boussif, O.; Lezoualc'h, F.; Zanta, M. A.; Mergny, M. D.; Scherman, D.; Demeneix, B.; Behr, J. P., A versatile vector for gene and oligonucleotide transfer into cells in culture and in vivo: polyethylenimine. *Proceedings of the National Academy of Sciences of the United States of America* **1995,** *92* (16), 7297-301.

26. Behr, J. P., The proton sponge: A trick to enter cells the viruses did not exploit. *Chimia* **1997,** *51* (1-2), 34-36.

27. Sonawane, N. D.; Szoka, F. C., Jr.; Verkman, A. S., Chloride accumulation and swelling in endosomes enhances DNA transfer by polyamine-DNA polyplexes. *The Journal of biological chemistry* **2003,** *278* (45), 44826-31.

28. Akinc, A.; Thomas, M.; Klibanov, A. M.; Langer, R., Exploring polyethylenimine-mediated DNA transfection and the proton sponge hypothesis. *The journal of gene medicine* **2005,** *7* (5), 657-63.

29. Godbey, W. T.; Wu, K. K.; Mikos, A. G., Size matters: molecular weight affects the efficiency of poly(ethylenimine) as a gene delivery vehicle. *Journal of biomedical materials research* **1999,** *45* (3), 268-75.

30. Fischer, D.; Li, Y.; Ahlemeyer, B.; Krieglstein, J.; Kissel, T., In vitro cytotoxicity testing of polycations: influence of polymer structure on cell viability and hemolysis. *Biomaterials* **2003,** *24* (7), 1121-31.

31. Neu, M.; Fischer, D.; Kissel, T., Recent advances in rational gene transfer vector design based on poly(ethylene imine) and its derivatives. *The journal of gene medicine* **2005,** *7* (8), 992-1009.

32. Dunlap, D. D.; Maggi, A.; Soria, M. R.; Monaco, L., Nanoscopic structure of DNA condensed for gene delivery. *Nucleic acids research* **1997,** *25* (15), 3095-101.

33. Reschel, T.; Konak, C.; Oupicky, D.; Seymour, L. W.; Ulbrich, K., Physical properties and in vitro transfection efficiency of gene delivery vectors based on complexes of DNA with synthetic polycations. *Journal of controlled release : official journal of the Controlled Release Society* **2002,** *81* (1-2), 201-17.

34. Tang, M. X.; Szoka, F. C., The influence of polymer structure on the interactions of cationic polymers with DNA and morphology of the resulting complexes. *Gene therapy* **1997,** *4* (8), 823-32.

35. Banerjee, P.; Reichardt, W.; Weissleder, R.; Bogdanov, A., Jr., Novel hyperbranched dendron for gene transfer in vitro and in vivo. *Bioconjugate chemistry* **2004,** *15* (5), 960-8.

36. Forrest, M. L.; Meister, G. E.; Koerber, J. T.; Pack, D. W., Partial acetylation of polyethylenimine enhances in vitro gene delivery. *Pharmaceutical research* **2004,** *21* (2), 365-71.

37. Zintchenko, A.; Philipp, A.; Dehshahri, A.; Wagner, E., Simple modifications of branched PEI lead to highly efficient siRNA carriers with low toxicity. *Bioconjugate chemistry* **2008,** *19* (7), 1448-55.

38. Kim, W. J.; Chang, C. W.; Lee, M.; Kim, S. W., Efficient siRNA delivery using water soluble lipopolymer for anti-anglogenic gene therapy. *Journal of Controlled Release* **2007,** *118* (3), 357-363.

39. Tamura, A.; Nagasaki, Y., Smart siRNA delivery systems based on polymeric nanoassemblies and nanoparticles. *Nanomedicine : nanotechnology, biology, and medicine* **2010,** *5* (7), 1089-1102.

40. Philipp, A.; Zhao, X. B.; Tarcha, P.; Wagner, E.; Zintchenko, A., Hydrophobically Modified Oligoethylenimines as Highly Efficient Transfection Agents for siRNA Delivery. *Bioconjugate chemistry* **2009,** *20* (11), 2055-2061.

41. Chen, J.; Tian, H. Y.; Guo, Z. P.; Xia, J. L.; Kano, A.; Maruyama, A.; Jing, X. B.; Chen, X. S., A Highly Efficient siRNA Carrier of PBLG Modified Hyperbranched PEI. *Macromol Biosci* **2009,** *9* (12), 1247-1253.

42. Mao, S.; Neu, M.; Germershaus, O.; Merkel, O.; Sitterberg, J.; Bakowsky, U.; Kissel, T., Influence of polyethylene glycol chain length on the physicochemical and biological properties of poly(ethylene imine)-graft-poly(ethylene glycol) block copolymer/SiRNA polyplexes. *Bioconjugate chemistry* **2006,** *17* (5), 1209-18.

43. Malek, A.; Merkel, O.; Fink, L.; Czubayko, F.; Kissel, T.; Aigner, A., In vivo pharmacokinetics, tissue distribution and underlying mechanisms of various PEI(-PEG)/siRNA complexes. *Toxicology and applied pharmacology* **2009,** *236* (1), 97-108.

44. Breunig, M.; Lungwitz, U.; Liebl, R.; Goepferich, A., Breaking up the correlation between efficacy and toxicity for nonviral gene delivery. *Proceedings of the National Academy of Sciences of the United States of America* **2007,** *104* (36), 14454-14459.

45. Kim, S. H.; Jeong, J. H.; Kim, T. I.; Kim, S. W.; Bull, D. A., VEGF siRNA Delivery System Using Arginine-Grafted Bioreducible Poly(disulfide amine). *Molecular pharmaceutics* **2009,** *6* (3), 718-726.

46. Matsumoto, S.; Christie, R. J.; Nishiyama, N.; Miyata, K.; Ishii, A.; Oba, M.; Koyama, H.; Yamasaki, Y.; Kataoka, K., Environment-Responsive Block Copolymer Micelles with a Disulfide Cross-Linked Core for Enhanced siRNA Delivery. *Biomacromolecules* **2009,** *10* (1), 119-127.

47. Giljohann, D. A.; Seferos, D. S.; Daniel, W. L.; Massich, M. D.; Patel, P. C.; Mirkin, C. A., Gold nanoparticles for biology and medicine. *Angewandte Chemie* **2010,** *49* (19), 3280-94.

48. Paciotti, G. F.; Myer, L.; Weinreich, D.; Goia, D.; Pavel, N.; McLaughlin, R. E.; Tamarkin, L., Colloidal gold: a novel nanoparticle vector for tumor directed drug delivery. *Drug delivery* **2004,** *11* (3), 169-83.

49. Mirkin, C. A.; Letsinger, R. L.; Mucic, R. C.; Storhoff, J. J., A DNA-based method for rationally assembling nanoparticles into macroscopic materials. *Nature* **1996,** *382* (6592), 607-609.

50. Dreaden, E. C.; Mackey, M. A.; Huang, X.; Kang, B.; El-Sayed, M. A., Beating cancer in multiple ways using nanogold. *Chem Soc Rev* **2011,** *40* (7), 3391-404.

51. Ghosh, P.; Han, G.; De, M.; Kim, C. K.; Rotello, V. M., Gold nanoparticles in delivery applications. *Advanced drug delivery reviews* **2008,** *60* (11), 1307-15.

52. Lal, S.; Clare, S. E.; Halas, N. J., Nanoshell-enabled photothermal cancer therapy: impending clinical impact. *Accounts of chemical research* **2008,** *41* (12), 1842-51.

53. Connor, E. E.; Mwamuka, J.; Gole, A.; Murphy, C. J.; Wyatt, M. D., Gold nanoparticles are taken up by human cells but do not cause acute cytotoxicity. *Small* **2005,** *1* (3), 325-7.

54. Skirtach, A. G.; Munoz Javier, A.; Kreft, O.; Kohler, K.; Piera Alberola, A.; Mohwald, H.; Parak, W. J.; Sukhorukov, G. B., Laser-induced release of encapsulated materials inside living cells. *Angewandte Chemie* **2006,** *45* (28), 4612-7.

55. Elbakry, A.; Zaky, A.; Liebl, R.; Rachel, R.; Goepferich, A.; Breunig, M., Layer-by-layer assembled gold nanoparticles for siRNA delivery. *Nano letters* **2009,** *9* (5), 2059-64.

56. Song, W. J.; Du, J. Z.; Sun, T. M.; Zhang, P. Z.; Wang, J., Gold nanoparticles capped with polyethyleneimine for enhanced siRNA delivery. *Small* **2010,** *6* (2), 239-46.

57. Lee, M. Y.; Park, S. J.; Park, K.; Kim, K. S.; Lee, H.; Hahn, S. K., Target-specific gene silencing of layer-by-layer assembled gold-cysteamine/siRNA/PEI/HA nanocomplex. *ACS nano* **2011,** *5* (8), 6138-47.

58. Lee, S. K.; Han, M. S.; Asokan, S.; Tung, C. H., Effective gene silencing by multilayered siRNA-coated gold nanoparticles. *Small* **2011,** *7* (3), 364-70.

59. Guo, S.; Huang, Y.; Jiang, Q.; Sun, Y.; Deng, L.; Liang, Z.; Du, Q.; Xing, J.; Zhao, Y.; Wang, P. C.; Dong, A.; Liang, X. J., Enhanced gene delivery and siRNA silencing by gold nanoparticles coated with charge-reversal polyelectrolyte. *ACS nano* **2010,** *4* (9), 5505-11.

60. von Maltzahn, G.; Park, J. H.; Agrawal, A.; Bandaru, N. K.; Das, S. K.; Sailor, M. J.; Bhatia, S. N., Computationally guided photothermal tumor therapy using long-circulating gold nanorod antennas. *Cancer research* **2009,** *69* (9), 3892-900.

61. Chithrani, B. D.; Ghazani, A. A.; Chan, W. C., Determining the size and shape dependence of gold nanoparticle uptake into mammalian cells. *Nano letters* **2006,** *6* (4), 662-8.

62. Jiang, W.; Kim, B. Y.; Rutka, J. T.; Chan, W. C., Nanoparticle-mediated cellular response is size-dependent. *Nature nanotechnology* **2008,** *3* (3), 145-50.

63. Giljohann, D. A.; Seferos, D. S.; Prigodich, A. E.; Patel, P. C.; Mirkin, C. A., Gene regulation with polyvalent siRNA-nanoparticle conjugates. *Journal of the American Chemical Society* **2009,** *131* (6), 2072-3.

64. Lee, J. S.; Green, J. J.; Love, K. T.; Sunshine, J.; Langer, R.; Anderson, D. G., Gold, poly(beta-amino ester) nanoparticles for small interfering RNA delivery. *Nano letters* **2009,** *9* (6), 2402-6.

65. Xia, W.; Low, P. S., Folate-targeted therapies for cancer. *Journal of medicinal chemistry* **2010,** *53* (19), 6811-24.

66. Leamon, C. P.; Low, P. S., Folate-mediated targeting: from diagnostics to drug and gene delivery. *Drug discovery today* **2001,** *6* (1), 44-51.

67. Lu, Y.; Low, P. S., Folate-mediated delivery of macromolecular anticancer therapeutic agents. *Advanced drug delivery reviews* **2002,** *54* (5), 675-93.

68. Antony, A. C., The biological chemistry of folate receptors. *Blood* **1992,** *79* (11), 2807-20.

69. Kamen, B. A.; Caston, J. D., Properties of a folate binding protein (FBP) isolated from porcine kidney. *Biochemical pharmacology* **1986,** *35* (14), 2323-9.

70. Ross, J. F.; Chaudhuri, P. K.; Ratnam, M., Differential regulation of folate receptor isoforms in normal and malignant tissues in vivo and in established cell lines. Physiologic and clinical implications. *Cancer* **1994,** *73* (9), 2432-43.

71. Shen, F.; Ross, J. F.; Wang, X.; Ratnam, M., Identification of a novel folate receptor, a truncated receptor, and receptor type beta in hematopoietic cells: cDNA

cloning, expression, immunoreactivity, and tissue specificity. *Biochemistry* **1994,** *33* (5), 1209-15.

72. Weitman, S. D.; Lark, R. H.; Coney, L. R.; Fort, D. W.; Frasca, V.; Zurawski, V. R., Jr.; Kamen, B. A., Distribution of the folate receptor GP38 in normal and malignant cell lines and tissues. *Cancer research* **1992,** *52* (12), 3396-401.

73. Low, P. S.; Antony, A. C., Folate receptor-targeted drugs for cancer and inflammatory diseases. *Advanced drug delivery reviews* **2004,** *56* (8), 1055-8.

74. Leamon, C. P.; Low, P. S., Delivery of macromolecules into living cells: a method that exploits folate receptor endocytosis. *Proceedings of the National Academy of Sciences of the United States of America* **1991,** *88* (13), 5572-6.

75. Leamon, C. P.; Jackman, A. L., Exploitation of the folate receptor in the management of cancer and inflammatory disease. *Vitamins and hormones* **2008,** *79*, 203-33.

76. Low, P. S.; Henne, W. A.; Doorneweerd, D. D., Discovery and development of folic-acid-based receptor targeting for imaging and therapy of cancer and inflammatory diseases. *Accounts of chemical research* **2008,** *41* (1), 120-9.

77. Reddy, J. A.; Allagadda, V. M.; Leamon, C. P., Targeting therapeutic and imaging agents to folate receptor positive tumors. *Current pharmaceutical biotechnology* **2005,** *6* (2), 131-50.

78. Choi, Y.; Thomas, T.; Kotlyar, A.; Islam, M. T.; Baker, J. R., Jr., Synthesis and functional evaluation of DNA-assembled polyamidoamine dendrimer clusters for cancer cell-specific targeting. *Chemistry & biology* **2005,** *12* (1), 35-43.

79. Choi, Y.; Baker, J. R., Jr., Targeting cancer cells with DNA-assembled dendrimers: a mix and match strategy for cancer. *Cell cycle* **2005,** *4* (5), 669-71.

80. Hwa Kim, S.; Hoon Jeong, J.; Chul Cho, K.; Wan Kim, S.; Gwan Park, T., Target-specific gene silencing by siRNA plasmid DNA complexed with folate-modified poly(ethylenimine). *Journal of controlled release : official journal of the Controlled Release Society* **2005,** *104* (1), 223-32.

81. Kim, S. H.; Mok, H.; Jeong, J. H.; Kim, S. W.; Park, T. G., Comparative evaluation of target-specific GFP gene silencing efficiencies for antisense ODN, synthetic siRNA, and siRNA plasmid complexed with PEI-PEG-FOL conjugate. *Bioconjugate chemistry* **2006,** *17* (1), 241-4.

82. Zhang, K.; Wang, Q.; Xie, Y.; Mor, G.; Sega, E.; Low, P. S.; Huang, Y., Receptor-mediated delivery of siRNAs by tethered nucleic acid base-paired interactions. *Rna* **2008,** *14* (3), 577-83.

83. Yoshizawa, T.; Hattori, Y.; Hakoshima, M.; Koga, K.; Maitani, Y., Folate-linked lipid-based nanoparticles for synthetic siRNA delivery in KB tumor xenografts. *European journal of pharmaceutics and biopharmaceutics : official journal of Arbeitsgemeinschaft fur Pharmazeutische Verfahrenstechnik e.V* **2008,** *70* (3), 718-25.

84. Zhang, Y. Folate Receptor-targeted delivery of small interfering RNA to cancer cells. University of Southern Mississippi, Hattiesburg, MS, 39401, 2010.

85. Brandenberger, C.; Muhlfeld, C.; Ali, Z.; Lenz, A. G.; Schmid, O.; Parak, W. J.; Gehr, P.; Rothen-Rutishauser, B., Quantitative evaluation of cellular uptake and trafficking of plain and polyethylene glycol-coated gold nanoparticles. *Small* **2010,** *6* (15), 1669-78.

86. Leon-Tamariz, F.; Verbaeys, I.; Van Boven, M.; De Cuyper, M.; Buyse, J.; de Witte, P.; Verbruggen, A.; Cokelaere, M., Biodistribution and pharmacokinetics of PEG-10kDa-cholecystokinin-10 in rats after different routes of administration. *Current drug delivery* **2010,** *7* (2), 137-43.

87. Ding, H. M.; Ma, Y. Q., Role of physicochemical properties of coating ligands in receptor-mediated endocytosis of nanoparticles. *Biomaterials* **2012,** *33* (23), 5798-802.

88. Patel, P. C.; Giljohann, D. A.; Daniel, W. L.; Zheng, D.; Prigodich, A. E.; Mirkin, C. A., Scavenger receptors mediate cellular uptake of polyvalent oligonucleotide-functionalized gold nanoparticles. *Bioconjugate chemistry* **2010,** *21* (12), 2250-6.

89. Zhang, Z.; Huey Lee, S.; Feng, S. S., Folate-decorated poly(lactide-co-glycolide)-vitamin E TPGS nanoparticles for targeted drug delivery. *Biomaterials* **2007,** *28* (10), 1889-99.

90. Zhang, Z.; Jia, J.; Lai, Y.; Ma, Y.; Weng, J.; Sun, L., Conjugating folic acid to gold nanoparticles through glutathione for targeting and detecting cancer cells. *Bioorganic & medicinal chemistry* **2010,** *18* (15), 5528-34.

91. Xiao, Z.; Ji, C.; Shi, J.; Pridgen, E. M.; Frieder, J.; Wu, J.; Farokhzad, O. C., DNA self-assembly of targeted near-infrared-responsive gold nanoparticles for cancer thermo-chemotherapy. *Angewandte Chemie* **2012,** *51* (47), 11853-7.

92. de Oliveira, R.; Zhao, P.; Li, N.; de Santa Maria, L. C.; Vergnaud, J.; Ruiz, J.; Astruc, D.; Barratt, G., Synthesis and in vitro studies of gold nanoparticles loaded with docetaxel. *International journal of pharmaceutics* **2013,** *454* (2), 703-11.